Non-Markovian optimal sideband cooling

Cite as: AIP Conference Proceedings **1950**, 030004 (2018); https://doi.org/10.1063/1.5031696
Published Online: 18 April 2018

Johan F. Triana, and Leonardo A. Pachon

Non-Markovian Optimal Sideband Cooling

Johan F. Triana and Leonardo A. Pachon[a),b)]

Grupo de Física Atómica y Molecular and Grupo de Física Teórica y Matemática Aplicada, Instituto de Física, Facultad de Ciencias Exactas y Naturales, Universidad de Antioquia UdeA; Calle 70 No. 52-21, Medellín, Colombia.

[a)]Corresponding author: leonardo.pachon@udea.edu.co
[b)]URL: http://gfam.udea.edu.co/~lpachon/

Abstract. Optimal control theory is applied to sideband cooling of nano-mechanical resonators. The formulation described here makes use of exact results derived by means of the path-integral approach of quantum dynamics, so that no approximation is invoked. It is demonstrated that the intricate interplay between time-dependent fields and structured thermal bath may lead to improve results of the sideband cooling by an order of magnitude. Cooling is quantified by means of the mean number of phonons of the mechanical modes as well as by the von Neumann entropy. Potencial extension to non-linear systems, by means of semiclassical methods, is briefly discussed.

INTRODUCTION

Mechanical micro- and nano-resonators cooled to very low temperatures can be used to explore quantum effects such as superposition of states, entanglement at macroscopic scales [1] and, when non-Markovian interactions are considered, thermal equilibrium states different from the canonical Boltzmann distribution [2]. Additionally, when they are coupled to optical systems or superconducting qubits at low temperatures, they can be used for performing ultra precise measurements [3, 4], detecting gravitational waves [5] or as a tool for studying fundamental issues such as the quantum-mechanical transition [6]. However, in the case of nanoresonators, e.g., the frequency of operation is in the range of 1 MHz to 1 GHz. For this range of frequencies, the quantum nature of the resonator will only be unveiled if the temperature is below 10 μK and 10 mK, respectively [7]. The nature and complexity of the problem becomes evident when it is noticed that a cryostat only reaches temperatures of the order of 10 mK [8]. Given the importance and relevance of these systems at low temperatures, recently, there have been developed [1, 5, 8, 9] and proposed [10, 11] multiple techniques that will allow to bring these resonators to excitation levels near to the ground state.

The time scales where cooling takes place are very short, of the order of the resonator period, and the temperature involved in the process is very low; therefore, it is then expected that non-Markovian effects, arising form the resonator and its environment interaction, dominate the transfer of energy and entropy between them [10, 12, 13]. However, recently proposed schemes [11, 14, 15, 16, 17, 18] have been all performed under the assumption of Markovian dynamics. So that, it is fair to say that a complete understanding of the cooling process is still under construction. Therefore, in designing more robust techniques and analyzing all previous schemes [1, 5, 8, 9], it is necessary to consider the effects of non-Markovian dynamics. To be sure, the role of non-Markovian dynamics in cooling process has been studied in other physical systems like spins with very positive results [12, 13].

This work starts with the standard derivation of the Hamiltonian model [19, 20]. To quantify the effects of non-Markovian interactions in the minimum phonon number at equilibrium, memory effects in the equations of motion for the mechanical and optical modes are introduced next. Later, optimal control theory is applied to sideband cooling to find an optimal control pulse to get (i) the minimum phonon number, under Markovian and non-Markovian dynamics, and (ii) to maintain the minimum phonon number once it is reached. Finally, the squeezing generation and entropy transfer during the cooling protocol are analyzed. The results obtained in this part justify the use the number of phonons in the mechanical mode as the cooling measure.

Latin-American School of Physics Marcos Moshinsky ELAF2017
AIP Conf. Proc. 1950, 030004-1–030004-20; https://doi.org/10.1063/1.5031696
Published by AIP Publishing. 978-0-7354-1645-1/$30.00

MODEL

Cavity optomechanics focuses on the study of the interaction between electromagnetic radiation and mechanical systems. Light is typically confined to a volume separated by two mirrors, in the case of optomechanical systems; or plates, in the case of electromechanical systems. Since one of the mirrors or plates can move, coupling between light and matter is mediated by radiation pressure (see below). This setup can be used for different applications, e.g., to obtain quantum effects in a nano-resonator that has around 10^{14} atoms, i.e., to reach phenomena predicted by quantum mechanics in the regime of mesoscopic objects.

The starting point is the standard derivation of the Hamiltonian [19, 20] that describes the mechanical system coupled to a radiation mode. The two modes are represented by two harmonic oscillators, one for the cavity or electromagnetic mode with and angular frequency $\omega_{\rm cav}$ and other for the vibrational or mechanical mode with angular frequency $\omega_{\rm m}$. Hence, the typical energy scale of the optical and mechanical mode are $\hbar\omega_{\rm cav}$ and $\hbar\omega_{\rm m}$, respectively. To derive the Hamiltonian in absence of thermal fluctuations and dissipation, consider the most common optomechanical system analyzed in the literature and successfully used in the experiments to date, namely, the Fabry-Perot cavity [11, 15, 18, 21, 22, 20, 23, 24, 25] (see Fig. 1). There, the end-mirror is moveable and corresponds to the vibrational or mechanical mode. Therefore, the Hamiltonian reads

$$\hat{H}_0 = \hbar\omega_{\rm m}\hat{a}^\dagger\hat{a} + \hbar\omega(\hat{x})\hat{b}^\dagger\hat{b}. \tag{1}$$

Because to the end-mirror is moving continuously, the coupling between optical and mechanical mode is parametric, i.e., the cavity resonance frequency is modulated by the mechanical amplitude which changes with the displacement of the end-mirror. Hence, in the linear approximation, the cavity frequency reads[1]

$$\omega(\hat{x}) \approx \omega_{\rm cav}\hat{1} + G\hat{x} + ..., \tag{2}$$

where $\omega_{\rm cav}$ is the central frequency of the cavity Fabry Perot cavity of length L. The optical frequency shift per displacement is defined as $G = \omega_{\rm cav}/L$. Therefore, the second term in Eq. (1) is approximately given by

$$\hbar\omega(\hat{x})\hat{b}^\dagger\hat{b} \approx \hbar(\omega_{\rm cav} + G\hat{x})\hat{b}^\dagger\hat{b}, \tag{3}$$

where $\hat{x} = x_{\rm ZPF}(\hat{a} + \hat{a}^\dagger)$ with $x_{\rm ZPF} = \sqrt{\hbar/2m_0\omega_{\rm m}}$ the zero-point fluctuation amplitude of the mechanical oscillator.

The light-matter interaction term then reads [19, 20]

$$\hat{H}_{\rm int} = \hbar g_0\hat{b}^\dagger\hat{b}(\hat{a} + \hat{a}^\dagger), \tag{4}$$

where $g_0 = Gx_{\rm ZPF}$ is the vacuum optomechanical coupling strength. Because g_0 is formed by a part of the optical mode (G) and other from the mechanical mode ($x_{\rm ZPF}$), it quantifies the interaction between radiation (a single photon) with matter (a single phonon). Now, to avoid the time-dependent driving terms that arise from the laser pulse, it is appropriated to apply a unitary transformation of the form $\hat{U} = \exp(i\omega_{\rm L}\hat{b}^\dagger\hat{b}t)$ to change the description of the optical mode to a frame rotating at the laser frequency $\omega_{\rm L}$. This unitary transformation generates a new Hamiltonian of the form [19, 20]

$$\hat{H} = \hbar\Delta\hat{b}^\dagger\hat{b} + \hbar\omega_{\rm m}\hat{a}^\dagger\hat{a} + \hbar g_0\hat{b}^\dagger\hat{b}(\hat{a} + \hat{a}^\dagger), \tag{5}$$

where $\Delta = \omega_{\rm cav} - \omega_{\rm L}$ is the laser detuning. Consider now the linearized approximate description of cavity optomechanics ($\hat{b} = \overline{\alpha} + \delta\hat{b}$), so that the Hamiltonian is then given by

$$\begin{aligned}\hat{H} &= \hbar\Delta\hat{b}^\dagger\hat{b} + \hbar\omega_{\rm m}\hat{a}^\dagger\hat{a} + \hbar g_0[(\overline{\alpha} + \delta\hat{b})^\dagger(\overline{\alpha} + \delta\hat{b})](\hat{a} + \hat{a}^\dagger) \\ &= \hbar\Delta\hat{b}^\dagger\hat{b} + \hbar\omega_{\rm m}\hat{a}^\dagger\hat{a} + \hbar g_0(\overline{\alpha}^2 + \overline{\alpha}(\delta\hat{b} + \delta\hat{b}^\dagger) + \delta\hat{b}^\dagger\delta\hat{b})(\hat{a}^\dagger + \hat{a}),\end{aligned} \tag{6}$$

where $\overline{\alpha} = \left\langle\hat{b}\right\rangle$ is the average coherent amplitude of the cavity field and $\delta\hat{b}$ is the fluctuating term due to vacuum noise. In equation (6), the first term $\overline{\alpha}^2 = \langle\hat{b}^\dagger\hat{b}\rangle$ can be omitted because it corresponds to the average of the radiation pressure force, it can be seen as a displacement from the average of the radiation pressure force. The third term $\delta\hat{b}^\dagger\delta\hat{b}$ can be neglected because it is much smaller than the second term for a factor of $\overline{\alpha}$.

[1] For a formal Taylor expansion of function of an operator see, e.g., Ref. [26]

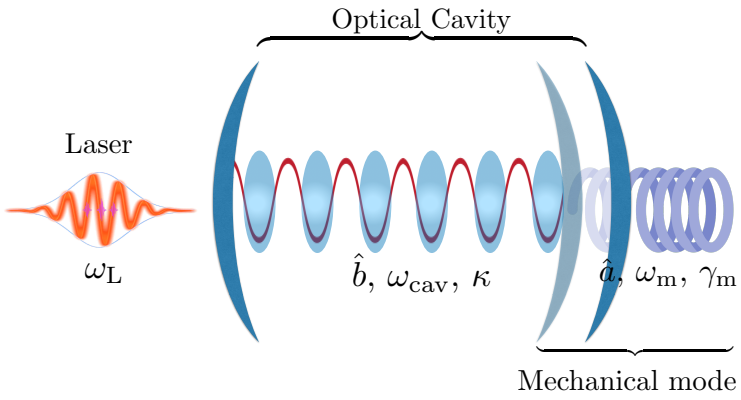

FIGURE 1: Schematic representation of a generic optomechanical system in the optical domain with a laser-driven optical cavity and a vibrating end mirror. ω_{L}, ω_{cav} and ω_{m} are the frequencies of the laser, cavity and mechanical resonator, respectively. κ and γ_{m} are the dissipation parameters of the cavity and mechanical resonator, respectively. The system consists of two mirrors, one of them is fixed and the end-mirror (mechanical mode) is moveable.

Therefore, the linearized Hamiltonian of the system reads [19, 20]

$$\hat{H} = \hbar\Delta\hat{b}^{\dagger}\hat{b} + \hbar\omega_{\mathrm{m}}\hat{a}^{\dagger}\hat{a} + \hbar g(\delta\hat{b}^{\dagger} + \delta\hat{b})(\hat{a} + \hat{a}^{\dagger}), \tag{7}$$

where $g = g_0\overline{\alpha}$ is the optomechanical coupling strength [15, 20]. The Hamiltonian described in Eq. (7) is the starting point to define the most important aspects in optomechanical systems [20]. These aspects depend explicitly on the system, the approximations in the Hamiltonian of Eq. (7) and the regimes which the system evolves. As for the system described above, the moveable end-mirror modulates the frequency of the cavity, i.e., the frequency of the cavity depends on the position of the end-mirror. This interplay between both systems is then generated by the oscillation of the mechanical mode which is called optomechanical "backaction" [20] (see schematic representation in Fig. 1).

Let us, for the moment, denote the dissipation rate of the cavity by κ and the dissipation rate of the mechanical mode by γ_{m}. Then, note that the dissipation rate of the cavity induces a delay between the motion and the changes of the radiation pressure force, this effect is known as "dynamical backaction" and is a fundamental phenomenon employed in the cooling process of the mechanical mode. Additionally, to reach a cooling process, the system has to be in the good cavity regime $\omega_{\mathrm{m}} > \gamma_{\mathrm{m}}$ and in the red-detuned regime $\Delta = \omega_{\mathrm{m}}$. Hence, if the rotating wave approximation is assumed valid, the linearized Hamiltonian of the system reads [20, 27]

$$\hat{H} = \hbar\Delta\hat{b}^{\dagger}\hat{b} + \hbar\omega_{\mathrm{m}}\hat{a}^{\dagger}\hat{a} + \hbar g(\hat{a}\delta\hat{b}^{\dagger} + \hat{a}^{\dagger}\delta\hat{b}). \tag{8}$$

The above conditions are those for achieving *sideband cooling* that have been extensively discussed in the literature [15, 21, 20, 23, 28, 29]. Sideband cooling has been described in optomechanical systems as well as in analogous systems such as electromechanical systems which use LC circuits and superconductors transmission lines coupled to a capacitor with a oscillating plate [20, 30, 31]. The capacitive coupling in these systems is to generate a dependence on the capacitance on the oscillating plate displacement to get the same change as in the Fabry-Perot cavity above. Hence, the Hamiltonian in Eq. (8) describes these electromechanical systems, so that the cooling protocol introduced here applies immediately to that kind of systems.

Minimum Phonon Number under Markovian and Non-Markovian Dynamics

The goal of this section is to derive the minimum phonon number as a function of the characteristics of the thermal bath to which the mechanical model is attached to. To make connections with previous cooling strategies, dissipative and decohering effects are considered here in a number of different alternatives ranging from quantum Langevin equations and adjoint master equations to path integrals. Covering the specific details of each alternative deviates the attention from the central aspects of this contribution. For this reason, details on the introduction of the non-unitary effects are provided only for the path-integral derivation of the dynamics in the Sec. *Sideband Cooling under Non-Markovian*

Evolution and appropriate references to other approaches are cited. In the present section, dissipative and decohering effects are introduced by means of a quantum Langevin equation, for details see Ref. [32, 33].

Thus, from the application of the quantum-optical Langevin formalism [32, 33] to the linearized Hamiltonian [Eq. (8)], the equations of motion for mechanical $\hat{a}(t)$ and optical $\hat{b}(t)$ modes read

$$\dot{\hat{a}}(t) = -\mathrm{i}\omega_{\mathrm{m}}\hat{a}(t) - \frac{1}{2}\int_0^t \mathrm{d}s\, \gamma(t-s)\hat{a}(s) - \mathrm{i}g(\hat{b}^\dagger + \hat{b}) - \sqrt{\gamma_{\mathrm{m}}}\hat{a}_{\mathrm{in}}(t), \tag{9}$$

$$\dot{\hat{b}}(t) = -\mathrm{i}\Delta\hat{b}(t) - \frac{1}{2}\int_0^t \mathrm{d}s\, \kappa(t-s)\hat{b}(s) - \mathrm{i}g(\hat{a}^\dagger + \hat{a}) - \sqrt{\kappa_{\mathrm{e}}/2}\hat{b}_{\mathrm{in}}(t) - \sqrt{\kappa_0}\hat{b}_{\mathrm{in,i}}(t). \tag{10}$$

κ_{e} and κ_0 are the rate associated to the input cooling and to the remaining loss rate, respectively, in the cavity mode. Similarly, $\hat{b}_{\mathrm{in}}$ and $\hat{b}_{\mathrm{in,i}}$ are the extrinsic and intrinsic fluctuating vacuum-electric-field operators coupled to the cavity responsible of the optical loss channels whereas $\hat{a}_{\mathrm{in}}$ is the noise operator that arises from the mechanical-system bath coupling. $\gamma(t)$ and $\kappa(t)$ are the dissipation kernels of the mechanical and cavity modes, respectively, which are discused below. Optomechanical cooling can be represented by the minimum phonon number in the mechanical mode. Hence, in the Fourier domain, the solution to Eqs. (9) and (10) is given by [18]

$$\hat{a}(\omega) = \frac{-\sqrt{\gamma_{\mathrm{m}}}\hat{a}_{\mathrm{in}}(\omega) - \mathrm{i}g(\hat{b}(\omega) + \hat{b}^\dagger(\omega))}{\mathrm{i}(\omega_{\mathrm{m}} - \omega) + \tilde{\gamma}_{\mathrm{m}}(\omega)/2}, \quad \hat{a}^\dagger(\omega) = \frac{-\sqrt{\gamma_{\mathrm{m}}}\hat{a}^\dagger_{\mathrm{in}}(\omega) + \mathrm{i}g(\hat{b}(\omega) + \hat{b}^\dagger(\omega))}{-\mathrm{i}(\omega_{\mathrm{m}} + \omega) + \tilde{\gamma}_{\mathrm{m}}(\omega)/2}, \tag{11}$$

$$\hat{b}(\omega) = \frac{-\sqrt{\kappa_{\mathrm{e}}/2}\hat{b}_{\mathrm{in}}(\omega) - \sqrt{\kappa_0}\hat{b}_{\mathrm{in,i}} - \mathrm{i}g(\hat{a}(\omega) + \hat{a}^\dagger(\omega))}{\mathrm{i}(\Delta - \omega) + \tilde{\kappa}(\omega)/2}, \quad \hat{b}^\dagger(\omega) = \frac{-\sqrt{\kappa_{\mathrm{e}}/2}\hat{b}^\dagger_{\mathrm{in}}(\omega) - \sqrt{\kappa_0}\hat{b}^\dagger_{\mathrm{in,i}} + \mathrm{i}g(\hat{a}(\omega) + \hat{a}^\dagger(\omega))}{-\mathrm{i}(\Delta + \omega) + \tilde{\kappa}(\omega)/2}, \tag{12}$$

where, using equations (11-12), the operator for the mechanical fluctuations reads

$$\hat{a}(\omega) = \frac{-\sqrt{\gamma_{\mathrm{m}}}\hat{a}_{\mathrm{in}}(\omega)}{\mathrm{i}(\tilde{\omega}_{\mathrm{m}} - \omega) + \tilde{\gamma}(\omega)/2} + \frac{\mathrm{i}g}{\mathrm{i}(\tilde{\omega}_{\mathrm{m}} - \omega) + \tilde{\gamma}(\omega)/2}\Big[\frac{\sqrt{\kappa_{\mathrm{e}}/2}\hat{b}_{\mathrm{in}}(\omega) + \sqrt{\kappa_0}\hat{b}_{\mathrm{in,i}}}{\mathrm{i}(\Delta - \omega) + \tilde{\kappa}(\omega)/2} + \frac{\sqrt{\kappa_0/2}\hat{b}^\dagger_{\mathrm{in}}(\omega) + \sqrt{\kappa_0}\hat{b}^\dagger_{\mathrm{in,i}}}{-\mathrm{i}(\Delta + \omega) + \tilde{\kappa}(\omega)/2}\Big], \tag{13}$$

where $\tilde{\omega}_{\mathrm{m}} = \omega_{\mathrm{m}} + \delta\omega_{\mathrm{m}}$ and $\tilde{\gamma} = \tilde{\gamma}_{\mathrm{m}} + \gamma_{\mathrm{OM}}$. The terms $\delta\omega_{\mathrm{m}}$ and γ_{OM} are the mechanical frequency shift and the optomechanical damping rate, respectively, due to the optical spring effect and are given by

$$\delta\omega_{\mathrm{m}} = |g|^2\mathrm{Im}\Big[\frac{1}{\mathrm{i}(\Delta - \omega_{\mathrm{m}}) + \tilde{\kappa}(\omega)/2} - \frac{1}{-\mathrm{i}(\Delta + \omega_{\mathrm{m}}) + \tilde{\kappa}(\omega)/2}\Big], \tag{14}$$

$$\gamma_{\mathrm{OM}} = 2|g|^2\mathrm{Re}\Big[\frac{1}{\mathrm{i}(\Delta - \omega_{\mathrm{m}}) + \tilde{\kappa}(\omega)/2} - \frac{1}{-\mathrm{i}(\Delta + \omega_{\mathrm{m}}) + \tilde{\kappa}(\omega)/2}\Big]. \tag{15}$$

It is worth mentioning that in Eq. (15), the maximum optical damping occurs in the red-detuned regime $\Delta = \omega_{\mathrm{m}}$ which coincides with the regime where the maximum cooling takes place (see below). For both Markovian and non-Markovian cases, the starting point to find the minimum phonon number is the quantum noise spectrum $S_{\mathrm{aa}}(\omega)$ of operator $\hat{a}$. This is defined next.

Quantum Noise Spectrum.—The optical mode is coupled to an optical bath that acts as a thermal bath with zero thermal occupation whereas the mechanical mode is coupled to a thermal bath that has an average phonon number $\overline{n}_{\mathrm{th}} \approx k_{\mathrm{B}}T/\hbar\omega_{\mathrm{m}}$. Considering that both modes are coupled to independent thermal baths, then the noise correlations associated to the input fluctuations are given by [18, 34]

$$\langle\hat{a}_{\mathrm{in}}(\omega)\hat{a}^\dagger_{\mathrm{in}}(\omega')\rangle = (\overline{n}_{\mathrm{th}} + 1)\delta(\omega + \omega'), \tag{16}$$

$$\langle\hat{a}^\dagger_{\mathrm{in}}(\omega)\hat{a}_{\mathrm{in}}(\omega')\rangle = \overline{n}_{\mathrm{th}}\delta(\omega + \omega'), \tag{17}$$

$$\langle\hat{b}_{\mathrm{in}}(\omega)\hat{b}^\dagger_{\mathrm{in}}(\omega')\rangle = \delta(\omega + \omega'), \tag{18}$$

$$\langle\hat{b}^\dagger_{\mathrm{in}}(\omega)\hat{b}_{\mathrm{in}}(\omega')\rangle = 0. \tag{19}$$

The quantum noise spectrum for the operator $\hat{a}$ given in Eq. (13) is defined as

$$S_{\mathrm{aa}}(\omega) = \int_{-\infty}^{\infty}\mathrm{d}\omega'\,\langle\hat{a}^\dagger(\omega)\hat{a}(\omega')\rangle, \tag{20}$$

so that, from Eqs. (13) and (20), the quantum noise spectrum is given by

$$S_{\mathrm{aa}}(\omega) = \frac{\tilde{\gamma}(\omega) n_{\mathrm{f}}(\omega)}{[\tilde{\gamma}(\omega)/2 - \mathrm{i}(\omega_{\mathrm{m}} + \omega)][\tilde{\gamma}(-\omega)/2 + \mathrm{i}(\omega_{\mathrm{m}} + \omega)]}, \tag{21}$$

being $n_{\mathrm{f}}(\omega)$ the the back-action modified phonon number. In terms of $\tilde{\gamma}(\omega)$ and $\tilde{\kappa}(\omega)$, $n_{\mathrm{f}}(\omega)$ reads

$$n_{\mathrm{f}}(\omega) = \frac{\gamma n_{\mathrm{b}}}{\tilde{\gamma}(\omega)} + \frac{g^2 \tilde{\kappa}(\omega)}{\tilde{\gamma}(\omega)} \left[\frac{1}{[\tilde{\kappa}(\omega)/2 - \mathrm{i}(\Delta - \omega)][\tilde{\kappa}(-\omega)/2 + \mathrm{i}(\Delta - \omega)]} \right]. \tag{22}$$

The dissipation kernel $\tilde{\gamma}(\omega)$ and $\tilde{\kappa}(\omega)$ are defined in terms of the spectral density (see next), which is a quantity that incorporates the nature and characteristics of the respective thermal baths and that can be reconstructed experimentally by means of spectroscopic techniques [35, 36].

Spectral Densities and Dissipation Kernels.—The spectral density $J_{\mathrm{D,C}}(\omega)$ defines the structure of the bath and provides the dissipation kernel by means of the relation

$$\gamma_{\mathrm{D,C}}(t) = \frac{2}{m} \int_0^\infty \frac{\mathrm{d}\omega}{\pi} \frac{J_{\mathrm{D,C}}(\omega)}{\omega} \cos(\omega t), \tag{23}$$

where $J_{\mathrm{D,C}}(\omega)$ denotes the most commonly used spectral densities with a cutoff frequency, namely, (i) the spectral density with a Drude cutoff frequency given by $J_{\mathrm{D}}(\omega) = m\gamma\omega\omega_{\mathrm{D}}^2/(\omega^2 + \omega_{\mathrm{D}}^2)$, and (ii) the Ohmic spectral density with a cutoff frequency ω_{C} given by $J_{\mathrm{C}}(\omega) = \gamma\omega \exp(-\omega/\omega_{\mathrm{C}})$. The Fourier transform of the dissipation kernels reads

$$\tilde{\gamma}_{\mathrm{D}}(\omega) = \frac{\gamma\omega_{\mathrm{D}}^2}{\omega^2 + \omega_{\mathrm{D}}^2}, \tag{24}$$

$$\tilde{\gamma}_{\mathrm{C}}(\omega) = \gamma \exp\left(-\frac{|\omega|}{\omega_{\mathrm{C}}}\right), \tag{25}$$

and the quantum noise spectrum finally is given by

$$S_{\mathrm{aa}}(\omega) = \frac{\tilde{\gamma}(\omega) n_{\mathrm{f}}(\omega)}{[\tilde{\gamma}(\omega)/2]^2 + (\omega_{\mathrm{m}} + \omega)^2}. \tag{26}$$

The back-action modified phonon number $n_{\mathrm{f}}(\omega)$ is given by

$$n_{\mathrm{f}}(\omega) = \frac{\gamma n_{\mathrm{b}}}{\tilde{\gamma}(\omega)} + \frac{g^2 \tilde{\kappa}(\omega)}{\tilde{\gamma}(\omega)} \left[\frac{1}{[\tilde{\kappa}(\omega)/2]^2 + (\Delta - \omega)^2} \right]. \tag{27}$$

From equation (27), the minimum phonon occupation number or the cooling limit is reached when the system is in the red-detuned regime ($\Delta = \omega_{\mathrm{m}}$) and the $n_{\mathrm{f}}(\omega)$ is evaluated at $\omega = -\omega_{\mathrm{m}}$.

Additionally, if it is assumed that the dissipation rate of the mechanical mode $\gamma \to 0$ and $n_{\mathrm{b}} = 0$ then, from Eqs. (15) and (27), the phonon number $n(\omega)$ and the optomechanical damping rate γ_{OM} result as

$$n(\omega) = \frac{g^2 \tilde{\kappa}(\omega)}{\gamma_{\mathrm{OM}}(\omega)} \left[\frac{1}{[\tilde{\kappa}(\omega)/2]^2 + 4\omega^2} \right], \tag{28}$$

$$\gamma_{\mathrm{OM}} = \frac{16 g^2 \tilde{\kappa}(\omega)\omega^2}{\tilde{\kappa}(\omega)^2 \{[\tilde{\kappa}(\omega)/2]^2 + 4\omega^2\}}. \tag{29}$$

Thus, the minimum phonon occupation number is given by

$$n_{\mathrm{min}}(\omega) = \frac{\tilde{\kappa}(\omega)^2}{16\omega^2}. \tag{30}$$

This result agrees with previous results in the Markovian case when $\omega_{\mathrm{D,C}} \to \infty$ [18, 20], for which $\tilde{\kappa}(\omega) = \gamma = \kappa$. In the non-Markovian regime, the cutoff frequency is of the order of the frequency of the mechanical mode. For the particular case when $\omega_{\mathrm{D,C}} = \omega_{\mathrm{m}}$ the Fourier transforms of the dissipation kernels in Eqs. (24) and (25) are

$$\tilde{\gamma}_{\mathrm{D}}(\omega) = \frac{\gamma}{2}, \quad \tilde{\gamma}_{\mathrm{C}}(\omega) = \frac{\gamma}{\mathrm{e}}. \tag{31}$$

Therefore, the Markovian minimum phonon occupation number $n_{\rm M}$, the non-Markovian minimum phonon occupation number with the Lorentzian spectral density $n_{\rm D}$, and the non-Markovian minimum phonon occupation number with the exponential spectral density $n_{\rm C}$, in the case $\gamma = \kappa$, are given by

$$n_{\rm M} = \frac{\kappa^2}{16\omega_{\rm m}^2}, \tag{32}$$

$$n_{\rm D} = \frac{1}{4}\left(\frac{\kappa^2}{16\omega_{\rm m}^2}\right) = 0.25 n_{\rm M}, \tag{33}$$

$$n_{\rm C} = \frac{1}{{\rm e}^2}\left(\frac{\kappa^2}{16\omega_{\rm m}^2}\right) \approx 0.135 n_{\rm M}. \tag{34}$$

The Markovian minimum phonon occupation $n_{\rm M}$ is obtained by taking the limit $\omega_{\rm D,C} \to \infty$ in the Fourier transforms of the dissipation kernel in Eqs. (24) and (25). Therefore, as it was discussed in Ref. [2], the quantum thermal equilibrium state depends explicitly on the structure of the environment and for the spectral densities considered here, that structure allows for reaching a lower minimum phonon number [see, Eqs. 33 and 34].

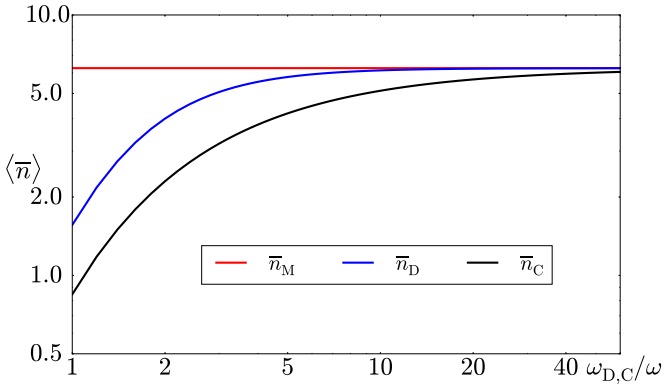

FIGURE 2: Minimum phonon number at equilibrium in terms of the cutoff frequency $\omega_{\rm D}$, which is considered as a measure of the non-Markovian character of the system. The dissipation parameter is $\kappa = 10^{-5}\omega$. The y-axis is scaled by 10^{-12}. Here, $n_{\rm M}$, $n_{\rm NML}$ and $n_{\rm NME}$ are the Markovian minimum phonon occupation number, the non-Markovian minimum phonon occupation number with the Lorentzian spectral density and the non-Markovian minimum phonon occupation number with the exponential spectral density, respectively.

Figure 2 shows the minimum phonon number obtained from Eq. (30) in terms of the cutoff frequency. As the cutoff frequency increases, the non-Markovian minimum phonon number approaches to the Markovian minimum phonon number. Hence, results in Eqs. (33) and (34) confirm that under non-Markovian dynamics the minimum phonon number is lower than in the Markovian case. However, to reach these lower phonon numbers, the system has to go through a dynamics that involve memory effects (non-Markovian). Therefore, the next step is to solve the dynamics of the system and apply optimal control theory to find the optical coupling function between the modes that allows for the larger transfer of entropy from the mechanical mode to the optical one, both in the Markovian as in the non-Markovian case.

SIDEBAND COOLING UNDER MARKOVIAN EVOLUTION

Recently, it was demonstrated that one can cool significantly better than traditional sideband cooling [11] by using quantum control based on steepest descent method [37]. In general, cooling is characterized by the average phonon number, $\langle \hat{n} \rangle = \langle \hat{a}^\dagger \hat{a} \rangle$. Because the system is linear, the dynamics is fully characterized by variances and covariances of the the ladder operators. As in Ref. [11], the equations of motion for the variances and covariances can be derived through the Markovian Brownian-motion master equation [11]. However, this set of equations violates the trace positivity of the density operator, in others words, the Markovian Brownian-motion master equation cannot be written in the Lindblad form (see, e.g., Chap. 3 in Ref. [38]).

For a first exploration here, a master equation in the Lindblad form is used, so that contrary to the equations of motion derived from the Brownian-motion master equation, the adjoint master equation used here obeys the positivity of the trace in the density operator. In deriving the adjoint master equation, it was assumed that the commutator of the Liouvillian of the dissipative dynamics and the Liouvillian of the driving force can be neglected provided that the time scale at which the system evolves is faster than the time scale of dissipative proceses. Note that if this is not the case, the adjoint mater equation is not formally valid [38]. In the path-integral description, there is no need of this assumption (see below).

Thus, the equation of motion of the variances of the position and momentum operators are found as follow. For the resonator and cavity, the position $\hat{q}_i$ and momentum $\hat{p}_i$ operators are given by $\hat{q}_{\rm m} = (\hat{a} + \hat{a}^\dagger)/\sqrt{2}$, $\hat{p}_{\rm m} = -{\rm i}(\hat{a} - \hat{a}^\dagger)/\sqrt{2}$, $\hat{q}_{\rm cav} = (\hat{b} + \hat{b}^\dagger)/\sqrt{2}$ and $\hat{p}_{\rm cav} = -{\rm i}(\hat{b} - \hat{b}^\dagger)/\sqrt{2}$, where the operators $\hat{q}_{\rm m}$ ($\hat{q}_{\rm cav}$) and $\hat{p}_{\rm m}$ ($\hat{p}_{\rm cav}$) correspond to the position and momentum operators of the mechanical (optical) mode. The Hamiltonian of the system in terms of the position and momentum reads

$$\hat{H}_{\rm S} = \sum_{i=1}^{2}\left(\frac{1}{2m_i}\hat{p}_i^2 + \frac{1}{2}m_i\omega_i\hat{q}_i^2\right) + g(t)\hat{q}_1\hat{q}_2, \tag{35}$$

where m_i and ω_i are the masses and frequencies of the modes. Once the Hamiltonian of the system is defined, the next step is to find the equations of motion for the second moments, in this case, in terms of the ladders operators. This set of equations is calculated using the Markovian adjoint master equation for a damped harmonic oscillator, which for an observable $A_{\rm H}$, in the Heisenberg picture, reads (see, e.g., Chap. 3 in Ref. [38])

$$\begin{aligned}\frac{\rm d}{{\rm d}t}A_{\rm H}(t) = {\rm i}\omega_{\rm m}[\hat{a}^\dagger\hat{a}, A_{\rm H}(t)] &+ \gamma(n_{\rm th}+1)\left\{\hat{a}^\dagger A_{\rm H}(t)\hat{a} - \frac{1}{2}\hat{a}^\dagger\hat{a}A_{\rm H}(t) - \frac{1}{2}A_{\rm H}(t)\hat{a}^\dagger\hat{a}\right\}\\ &+ \gamma n_{\rm th}\left\{\hat{a}A_{\rm H}(t)\hat{a}^\dagger - \frac{1}{2}\hat{a}\hat{a}^\dagger A_{\rm H}(t) - \frac{1}{2}A_{\rm H}(t)\hat{a}\hat{a}^\dagger\right\} + \kappa(n_{\rm cav}+1)\left\{\hat{b}^\dagger A_{\rm H}(t)\hat{b} - \frac{1}{2}\hat{b}^\dagger\hat{b}A_{\rm H}(t) - \frac{1}{2}A_{\rm H}(t)\hat{b}^\dagger\hat{b}\right\}\\ &+ \kappa n_{\rm cav}\left\{\hat{b}A_{\rm H}(t)\hat{b}^\dagger - \frac{1}{2}\hat{b}\hat{b}^\dagger A_{\rm H}(t) - \frac{1}{2}A_{\rm H}(t)\hat{b}\hat{b}^\dagger\right\}.\end{aligned} \tag{36}$$

γ and κ account for the non-unitary processes in the mechanical mode and optical mode, respectively. $n_{\rm th}$ ($n_{\rm cav}$) denotes the thermal occupation in the mechanical (optical) mode. Hence, the equations of motion of the second moments expectation values are given by

$$\dot{\langle\hat{a}\hat{a}\rangle}(t) = -2{\rm i}\omega_{\rm m}\langle\hat{a}\hat{a}\rangle + {\rm i}g(t)(\langle\hat{a}\hat{b}\rangle + \langle\hat{a}\hat{b}^\dagger\rangle) - \gamma\langle\hat{a}\hat{a}\rangle, \tag{37}$$

$$\dot{\langle\hat{a}\hat{a}^\dagger\rangle}(t) = -\frac{1}{2}{\rm i}g(t)\left(\langle\hat{b}^\dagger\hat{a}\rangle - \langle\hat{b}^\dagger\hat{a}^\dagger\rangle + \langle\hat{b}\hat{a}\rangle - \langle\hat{b}\hat{a}^\dagger\rangle\right) - \gamma(n_{\rm th}+1)\langle\hat{a}^\dagger\hat{a}\rangle + \gamma n_{\rm th}\langle\hat{a}\hat{a}^\dagger\rangle, \tag{38}$$

$$\dot{\langle\hat{a}\hat{b}\rangle}(t) = -2{\rm i}\omega_{\rm m}\langle\hat{a}\hat{b}\rangle + \frac{1}{2}{\rm i}g(t)\left(\langle\hat{b}\hat{b}\rangle + \langle\hat{a}\hat{a}\rangle + \langle\hat{b}^\dagger\hat{b}\rangle + \langle\hat{a}\hat{a}^\dagger\rangle\right) - \frac{1}{2}\gamma\langle\hat{a}\hat{b}\rangle - \frac{1}{2}\kappa\langle\hat{b}\hat{a}\rangle, \tag{39}$$

$$\dot{\langle\hat{a}\hat{b}^\dagger\rangle}(t) = \frac{1}{2}{\rm i}g(t)\left(\langle\hat{b}\hat{b}^\dagger\rangle - \langle\hat{a}\hat{a}^\dagger\rangle + \langle\hat{b}^\dagger\hat{b}^\dagger\rangle - \langle\hat{a}\hat{a}\rangle\right) - \frac{1}{2}\gamma\langle\hat{a}\hat{b}^\dagger\rangle - \frac{1}{2}\kappa\langle\hat{b}^\dagger\hat{a}\rangle, \tag{40}$$

$$\dot{\langle\hat{b}\hat{a}\rangle}(t) = -2{\rm i}\omega_{\rm m}\langle\hat{b}\hat{a}\rangle + \frac{1}{2}{\rm i}g(t)\left(\langle\hat{b}\hat{b}\rangle + \langle\hat{a}\hat{a}\rangle + \langle\hat{b}^\dagger\hat{b}\rangle + \langle\hat{a}\hat{a}^\dagger\rangle\right) - \frac{1}{2}\gamma\langle\hat{a}\hat{b}\rangle - \frac{1}{2}\kappa\langle\hat{b}\hat{a}\rangle, \tag{41}$$

$$\dot{\langle\hat{b}\hat{a}^\dagger\rangle}(t) = -\frac{1}{2}{\rm i}g(t)\left(\langle\hat{b}^\dagger\hat{b}\rangle - \langle\hat{a}^\dagger\hat{a}\rangle + \langle\hat{b}\hat{b}\rangle - \langle\hat{a}^\dagger\hat{a}^\dagger\rangle\right) - \frac{1}{2}\gamma\langle\hat{b}\hat{a}^\dagger\rangle - \frac{1}{2}\kappa\langle\hat{b}\hat{a}^\dagger\rangle, \tag{42}$$

$$\dot{\langle\hat{b}\hat{b}\rangle}(t) = -2{\rm i}\omega_{\rm m}\langle\hat{b}\hat{b}\rangle + {\rm i}g(t)(\langle\hat{b}\hat{a}\rangle + \langle\hat{b}\hat{a}^\dagger\rangle) - \kappa\langle\hat{b}\hat{b}\rangle, \tag{43}$$

$$\dot{\langle\hat{b}\hat{b}^\dagger\rangle}(t) = -\frac{1}{2}{\rm i}g(t)\left(\langle\hat{b}\hat{a}^\dagger\rangle - \langle\hat{b}^\dagger\hat{a}^\dagger\rangle + \langle\hat{b}\hat{a}\rangle - \langle\hat{b}^\dagger\hat{a}\rangle\right) - \kappa(n_{\rm cav}+1)\langle\hat{b}^\dagger\hat{b}\rangle + \kappa n_{\rm cav}\langle\hat{b}\hat{b}^\dagger\rangle, \tag{44}$$

$$\dot{\langle\hat{a}^\dagger\hat{a}\rangle}(t) = \frac{1}{2}{\rm i}g(t)\left(\langle\hat{b}\hat{a}^\dagger\rangle + \langle\hat{b}^\dagger\hat{a}^\dagger\rangle - \langle\hat{b}\hat{a}\rangle - \langle\hat{b}^\dagger\hat{a}\rangle\right) - \gamma(n_{\rm th}+1)\langle\hat{a}^\dagger\hat{a}\rangle + \gamma n_{\rm th}\langle\hat{a}\hat{a}^\dagger\rangle, \tag{45}$$

$$\langle \dot{\hat{a}^\dagger}\hat{a}^\dagger\rangle(t) = 2\mathrm{i}\omega_\mathrm{m}\langle \hat{a}^\dagger\hat{a}^\dagger\rangle - \mathrm{i}g(t)(\langle \hat{b}^\dagger\hat{a}^\dagger\rangle + \langle \hat{b}\hat{a}^\dagger\rangle) - \gamma\langle \hat{a}^\dagger\hat{a}^\dagger\rangle, \tag{46}$$

$$\langle \dot{\hat{a}^\dagger}\hat{b}\rangle(t) = -\frac{1}{2}\mathrm{i}g(t)\left(\langle \hat{b}^\dagger\hat{b}\rangle - \langle \hat{a}^\dagger\hat{a}\rangle + \langle \hat{b}\hat{b}\rangle - \langle \hat{a}^\dagger\hat{a}^\dagger\rangle\right) - \frac{\gamma}{2}\langle \hat{a}^\dagger\hat{b}\rangle - \frac{\kappa}{2}\langle \hat{a}^\dagger\hat{b}\rangle, \tag{47}$$

$$\langle \dot{\hat{a}^\dagger}\hat{b}^\dagger\rangle(t) = 2\mathrm{i}\omega_\mathrm{m}\langle \hat{a}^\dagger\hat{b}^\dagger\rangle - \frac{1}{2}\mathrm{i}g(t)\left(\langle \hat{a}^\dagger\hat{a}^\dagger\rangle + \langle \hat{b}^\dagger\hat{b}^\dagger\rangle + \langle \hat{b}\hat{b}^\dagger\rangle + \langle \hat{a}^\dagger\hat{a}\rangle\right) - \frac{1}{2}\gamma\langle \hat{a}^\dagger\hat{b}^\dagger\rangle - \frac{1}{2}\kappa\langle \hat{b}^\dagger\hat{a}^\dagger\rangle, \tag{48}$$

$$\langle \dot{\hat{b}^\dagger}\hat{a}\rangle(t) = \frac{1}{2}\mathrm{i}g(t)\left(\langle \hat{b}\hat{b}^\dagger\rangle - \langle \hat{a}\hat{a}^\dagger\rangle + \langle \hat{b}^\dagger\hat{b}^\dagger\rangle - \langle \hat{a}\hat{a}\rangle\right) - \frac{1}{2}\gamma\langle \hat{b}^\dagger\hat{a}\rangle - \frac{1}{2}\kappa\langle \hat{a}\hat{b}^\dagger\rangle, \tag{49}$$

$$\langle \dot{\hat{b}^\dagger}\hat{a}^\dagger\rangle(t) = 2\mathrm{i}\langle \hat{b}^\dagger\hat{a}^\dagger\rangle - \frac{1}{2}\mathrm{i}g(t)\left(\langle \hat{a}^\dagger\hat{a}^\dagger\rangle + \langle \hat{b}^\dagger\hat{b}^\dagger\rangle + \langle \hat{b}\hat{b}^\dagger\rangle + \langle \hat{a}^\dagger\hat{a}\rangle\right) - \frac{1}{2}\gamma\langle \hat{b}^\dagger\hat{a}^\dagger\rangle - \frac{1}{2}\kappa\langle \hat{a}^\dagger\hat{b}^\dagger\rangle, \tag{50}$$

$$\langle \dot{\hat{b}^\dagger}\hat{b}\rangle(t) = \frac{1}{2}\mathrm{i}g(t)\left(\langle \hat{b}^\dagger\hat{a}\rangle + \langle \hat{b}^\dagger\hat{a}^\dagger\rangle - \langle \hat{b}\hat{a}\rangle - \langle \hat{b}\hat{a}^\dagger\rangle\right) - \kappa(n_\mathrm{cav}+1)\langle \hat{b}^\dagger\hat{b}\rangle + \kappa n_\mathrm{cav}\langle \hat{b}\hat{b}^\dagger\rangle, \tag{51}$$

$$\langle \dot{\hat{b}^\dagger}\hat{b}^\dagger\rangle(t) = 2\mathrm{i}\omega_\mathrm{m}\langle \hat{b}^\dagger\hat{b}^\dagger\rangle - \mathrm{i}g(t)(\langle \hat{b}^\dagger\hat{a}^\dagger\rangle + \langle \hat{b}^\dagger\hat{a}\rangle) - \kappa\langle \hat{b}^\dagger\hat{b}^\dagger\rangle. \tag{52}$$

Optimal control theory is introduced next to find the coupling function $g(t)$ that minimizes the phonon number in the resonator.

Optimal Control Theory Applied to Sideband Cooling

Optimal control theory has been well developed for over forty years to improve the efficiency of different kind of systems or situations under a control parameter [37]. The advances of computer facilities make that optimal control is now widely used in multi-disciplinary applications such as biological systems, communication networks and socio-economic systems [39, 40, 41, 42]. The objective of optimal control theory is to determine the control of signals that will cause a process to satisfy the physical constraints and at the same time minimizes some performance criterion. This design is generally done by a trial-and-error process in which various methods of analysis are used iteratively to determine the design parameters of an "aceptable" system. Acceptable performance is generally defined in terms of time and frequency domain criteria such as rise time, settling time, peak overshoot and bandwidth.

To get an idea of how optimal control theory works, the problem at hand has to be formulated following three specific steps:

1. Mathematical description (or model) of the process to be controlled, i.e., the description of the system in terms of n first-order differential equations, as a state vector of the system $\boldsymbol{x}(t)$ and the control vector $\boldsymbol{u}(t)$. Hence, the state equations can be written as
$$\dot{\boldsymbol{x}} = \boldsymbol{a}(\boldsymbol{x}(t), \boldsymbol{u}(t), t). \tag{53}$$
2. A statement of the physical constraints, i.e., the initial (final) conditions of the system constraints $\boldsymbol{x}(t_0)$.
3. Specification of the physical criterion to minimize or maximize given by
$$J = h[\boldsymbol{x}(t), t] + \int_0^{t_\mathrm{f}} \mathrm{d}t\, V[\boldsymbol{x}(t), \boldsymbol{u}(t), t], \tag{54}$$
where $h\,[\mathbf{x}(t), t]$ and $V\,[\mathbf{x}(t), \mathbf{u}(t), t]$ are arbitrary functions, $\mathbf{x}(t)$ and $\mathbf{u}(t)$ are the vector of the equations of motion and the vector of the optimal functions, respectively.

Once the problem has been formally formulated, optimal control theory is aimed at solving the following problem. Find a control function $\boldsymbol{u}^\star$ that causes the system described by Eq. (53) follows the behaviour $\boldsymbol{x}^\star$ that minimizes the condition in Eq. (54). Here $\boldsymbol{u}^\star$ is called the *optimal control* and $\boldsymbol{x}^\star$ is called the *optimal trajectory*. Note that, even, if an optimal control exists, it may not be unique. The optimal control function may depend upon the initial condition of the control function, i.e., one should explore different initials parameters for not to fall in a local minimum but to reach the global minimum of the condition to minimize J.

As mentioned above, optimal control theory has been used in many disciplines with different algorithms or methodologies. In the cooling context, two previous investigations are pioneers in the optimal cooling of open quantum systems and the effects of the driving [10, 11]. In summary, the problem consists in finding an optimal coupling

function between a nano-mechanical resonator and a cavity mode to obtain the minimum phonon number in the Markovian as well as in the non-Markovian case.

To find the minimum phonon number in the mechanical mode under Markovian dynamics, Eqs. (37-52) are solved under the condition that

$$J = \left\langle \hat{a}^\dagger \hat{a} \left[\mathbf{x}(t), t \right] \right\rangle \tag{55}$$

is minimum. Thus, the minimization criterium only depends on the state vector of the system. Hence, in Eq. (54), $V\left[\mathbf{x}(t), \mathbf{u}(t), t\right] = 0$, $h\left[\mathbf{x}(t), t\right] = \left\langle \hat{a}^\dagger \hat{a} \left[\mathbf{x}(t), t\right] \right\rangle$ and $\mathbf{u}(t) = g(t)$ being $g(t)$ the total coupling function. To calculate the costate equations [see Eq. (57) below], an auxiliary Hamiltonian H_{OPT} is defined as $H_{\mathrm{OPT}} = \mathbf{p} \cdot \mathbf{x}$, being $\mathbf{p}$ the vector of the costate equations, which is explained in more detail below.

The algorithm used to solve the optimization problem, in the Markovian as well as in non-Markovian case, is the method of steepest descent [37]. It consists in the following steps:

1. Subdivide the interval $[t_0, t_f]$ into N equal subintervals and assume an initial piecewise-constant control $g^{(0)}(t) = g(0)(t_k)$, $t \in [t_k, t_{k+1}]$ $k = 0, 1, ..., N-1$. In this case, the control function is the coupling function $g(s)$ and the vector of the optimal functions is composed by one function.
2. Apply the assumed control $g^{(i)}$ to integrate the state equations from t_0 to t_{cool} with initial conditions $\mathbf{x}(t_0) = \mathbf{x}_0$ and store the state trajectory $\mathbf{x}^{(i)}$. Eqs. (37)-(52) are solved and the state trajectory is stored to modify the control function.
3. Apply $g^{(i)}$ and $\mathbf{x}^{(i)}$ to integrate costate equations backward in time, i.e., from $[t_{\mathrm{cool}}, t_0]$. The "initial value" $\mathbf{p}^{(i)}(t_{\mathrm{cool}})$ is obtained by:

$$\mathbf{p}^{(i)}(t_{\mathrm{cool}}) = \frac{\partial \left\langle \hat{a}^\dagger \hat{a} \left[\mathbf{x}^{(i)}(t_{\mathrm{cool}}) \right] \right\rangle}{\partial \mathbf{x}}, \tag{56}$$

   and according to optimal control theory, the costate equations to solve backward in time are calculated by

$$\dot{\mathbf{p}} = -\frac{\partial H_{\mathrm{OPT}}}{\partial \mathbf{x}}. \tag{57}$$

   After integrating the costate equations, $\partial H^{(i)}_{\mathrm{OPT}}(t)/\partial g$, $t \in [t_0, t_{\mathrm{cool}}]$ is evaluated and stored.
4. If

$$\left\| \frac{\partial H^{(i)}_{\mathrm{OPT}}}{\partial g} \right\| \leq \epsilon, \tag{58}$$

$$\left\| \frac{\partial H^{(i)}_{\mathrm{OPT}}}{\partial g} \right\|^2 \equiv \int_{t_0}^{t_f} \left[\left\| \frac{\partial H^{(i)}_{\mathrm{OPT}}}{\partial g} \right\| \right]^T \left[\left\| \frac{\partial H^{(i)}_{\mathrm{OPT}}}{\partial g} \right\| \right] \mathrm{d}t, \tag{59}$$

   then stop the iterative procedure. Here ϵ is a preselected small positive constant used as a tolerance. If Eq. (58) is not satisfied, adjust the control function as

$$g^{(i+1)}(t) = g^{(i)}(t) - \tau \frac{\partial H^{(i)}_{\mathrm{OPT}}}{\partial g}(t), \tag{60}$$

   and replace $g^{(i)}$ by $g^{(i+1)}$ and return to step 2. Here, τ is the step size to adjust the control function.

Results for optimal sideband cooling under Markovian evolution are shown in Fig. 3. The inset there shows two coupling functions: (i) the blue curve depicts the optimal coupling function $g_{\mathrm{opt}}(t)$ found with the equations of motion derived from the adjoint master equation in the Lindblad form and (ii) the red curve depicts the optimal coupling function $g(t)$ found with the equation of motions derive from the Brownian-motion master equation found in Ref. [11]. The limits of the coupling function $g_{\mathrm{opt}}(t)$ are the double of the function coupling $g(t)$. Despite the inadequateness of the Brownian master equation, it seems that the only noticeable effect is a scaling factor of the field. Additionally, Figure 3 shows the results for the minimum phonon number $\overline{n} = \langle \hat{a}^\dagger \hat{a} \rangle$ as a function of time for a number of values of the dissipation rate. To compare with results from Ref. [11], the time at which the minimum phonon number in the resonator is obtained is $t_{\mathrm{f}} = t_{\mathrm{cool}} = 0.55\tau_{\mathrm{m}}$, being τ_{m} the period of the mechanical mode. As the dissipation rate of the mechanical mode increases, the efficiency of the cooling protocol is undermined and the minimum phonon number may remain far from that of the ground state.

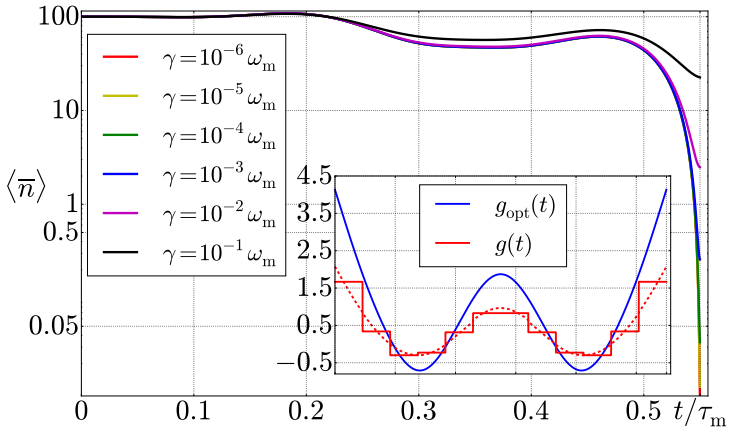

FIGURE 3: Cooling dynamics with the equations of motion derived using the adjoint master equation for different parameters of dissipation. The initial parameters are $n_{\rm th} = 100$, $n_{\rm cav} = 0$, $\kappa = 2.15\times10^{-4}\omega_0$. Inset: The optimal control pulse for the coupling rate $g_{\rm opt}(t)$ and the optimal 12-segment piecewise-constant control pulse for the coupling rate $g(t)$ (red line) and the coupling function $g(t)$ found by [11] (red dashed lines). The y-axis is in logarithmic scale.

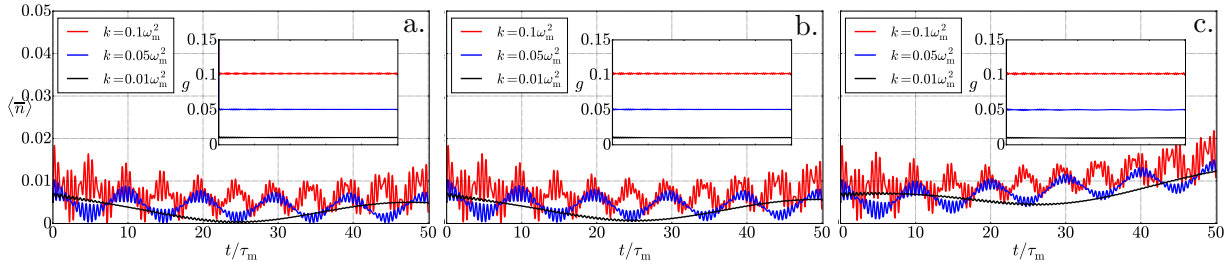

FIGURE 4: Phonon number as a function of time during the optimal control protocol aimed at maintaing the minimum phonon number for different parameters of dissipation (a) $\gamma = 10^{-6}\omega_{\rm m}$, (b) $\gamma = 10^{-5}\omega_{\rm m}$ and (c) $\gamma = 10^{-4}\omega_{\rm m}$. The common initial parameters are $n_{\rm th} = 100$, $n_{\rm cav} = 0$, $\kappa = 2.15\times10^{-4}\omega_{\rm m}$. Insets: The optimal control pulse for the coupling rate $g(t)$.

Optimal Control to Maintain the Minimum Phonon Number

Reaching a very low phonon number in a short period of time is a very desirable goal; however, since the resonator is continuously coupled to its environment, keeping that phonon number is a challenge. Therefore, the next step is to find the optimal coupling function that keeps phonon the number as close as possible to the minimum one obtained in the cooling protocol. Specifically, optimal control theory is used to maintain the minimum phonon number for about fifty periods of the resonator. To do so, the initial coupling function is chosen as a decaying exponential function which tends to a constant value k given by

$$g_{\rm m}(t) = e^{-\alpha t} + k, \tag{61}$$

where α is the decay factor that should be large enough to prevent the system to recover the entropy released into the optical mode. Details are discussed elsewhere [43].

In Figure 4, for a variety of different parameters of dissipation ($\gamma = 10^{-6}\omega_{\rm m}$, $\gamma = 10^{-5}\omega_{\rm m}$, $\gamma = 10^{-4}\omega_{\rm m}$), it is seen that lowest phonon number corresponds to that with the smallest k factor. Despite of the control protocol, when dissipation increases, the minimum phonon number also increases. Parameters in Fig. 4 are typical for some optomechanical systems such as microwave superconducting cavities, which operates in the GHz regime at temperature of the order of millikelvins [44, 45]. Further, current experiments with nanomechanical resonators have these typical parameters: $\omega_{\rm m} = 2\pi\times 15$ MHz, $m = 10^{-17}$ kg, $g \sim 10^{-3}\omega_{\rm m}^2$, and a quality factor $Q \sim 20000$, which yields a damping $\gamma = 5\times10^{-5}\omega_{\rm m}$ [46]. Thus, results in Fig. 4 are relevant at the experimental side.

Hence, the entire cooling process encompasses two processes: (i) reaching the minimum phonon number (see

Fig. 3) and (ii) keeping that minimum phonon number (see Fig. 4). Therefore, the optimal pulse $g_{\rm m}^{\star}(t)$ obtained from Eq. (61) is the continuation of the optimal pulse to cool showed in Fig. 3. Thus, it takes into account that the minimum phonon number is reached approximately at $t_{\rm cool} = 0.55\tau_{\rm m}$ and the optimal pulse as [27]

$$c(t) = \begin{cases} g(t) & 0 \leq t \leq 0.55\tau_{\rm m} \\ g_{\rm m}^{\star}(t) & t > 0.55\tau_{\rm m} \end{cases} . \tag{62}$$

The next step is to perform the optimal cooling process including non-Markovian interactions. As it is mentioned above, when compared to results from the Markovian approximation, the minimum phonon number at equilibrium is lower when the non-Markovian interactions are taking into account. Therefore, it is expected to have a similar phenomenon in the out of equilibrium regime.

Sideband Cooling Under Non-Markovian Evolution

To solve the dynamics in the non-Markovian regime, the influence functional theory by Feynman-Vernon is employed [47, 48, 49]. It allows for the study of the dynamics in open quantum systems without the rotating wave approximation (RWA) nor Markovian approximation [50, 51, 52]. So that a description of the system without any approximation can be performed, i.e., a full description of the non-Markovian dynamics. As above, the mechanical and the optical modes are coupled to independent thermal baths described by the Caldeira-Leggett model [53, 54, 55]. The complete Hamiltonian of the system (system+baths) is given by

$$\hat{H} = \sum_{i=1}^{2}\left(\frac{1}{2m_i}\hat{p}_i^2 + \frac{1}{2}m_i\omega_i^2\hat{q}_i^2\right) - c(t)q_1q_2 + \sum_{\mathrm{j},\alpha}^{\mathfrak{N},2}\left[\frac{\hat{p}_{\mathrm{j},\alpha}^2}{2m_{\mathrm{j},\alpha}} + \frac{m_{\mathrm{j},\alpha}\omega_{\mathrm{j},\alpha}^2}{2}\left(\hat{q}_{\mathrm{j},\alpha} - \frac{c_{\mathrm{j},\alpha}}{m_{\mathrm{j},\alpha}\omega_{\mathrm{j},\alpha}^2}\hat{q}_\alpha\right)^2\right], \tag{63}$$

with $\alpha = \{1, 2\}$, where the coefficients $c_{\mathrm{j},\alpha}$ are the coupling constants among each mode of the system of interest with their own thermal bath modes, $m_{\mathrm{j},\alpha}$ and $\omega_{\mathrm{j},\alpha}$ are the masses and frequencies of each mode of each thermal bath, respectively.

In solving the dynamics, initial correlations between coupled oscillators $\hat{\rho}_{\rm S}$ and their thermal baths $\hat{\rho}_{{\rm TB}_\alpha}$ are neglected [55], i.e., the total initial density operator is assumed to be given by

$$\hat{\rho}(0) = \hat{\rho}_{\rm S}(0) \otimes \hat{\rho}_{{\rm TB}_1} \otimes \hat{\rho}_{{\rm TB}_2}. \tag{64}$$

Additionally, the initial density matrix of the baths is taken as $\hat{\rho}_{{\rm TB}_\alpha}(0) = e^{-\beta_\alpha \hat{H}_{{\rm B}\alpha}}/Z_{{\rm TB}_i}$ at inverse temperatures $\beta_\alpha = 1/k_{\rm B}T_\alpha$. In this expression, $Z_{{\rm TB}_\alpha}$ denotes the partition function of each bath. Following the influence functional approach, the state of the mechanical and the optical mode $\hat{\rho}_{\rm S}(q''_{1+}, q''_{2+}, q''_{1-}, q''_2, t)$ can be determined from

$$\begin{aligned}\hat{\rho}_S(q''_{1+}, q''_{2+}, q''_{1-}, q''_2, t) = &\int_{-\infty}^{\infty} {\rm d}q'_{1+}{\rm d}q'_{2+}{\rm d}q'_{1-}{\rm d}q'_{2-}\, J(q''_{1+}, q''_{2+}, q''_{1-}, q''_{2-}, t; q'_{1+}, q'_{2+}, q'_{1-}, q'_{2-}, 0) \\ &\times \hat{\rho}_{\rm S}(q'_{1+}, q'_{2+}, q'_{1-}, q'_{2-}, 0),\end{aligned} \tag{65}$$

where $\rho_{\rm S}(q'_{1+}, q'_{2+}, q'_{1-}, q'_{2-}, 0)$ accounts for the initial state and $J(q''_{1+}, q''_{2+}, q''_{1-}, q''_{2-}, t; q'_{1+}, q'_{2+}, q'_{1-}, q'_{2-}, 0)$ is the propagating function. As each mode is coupled to its own Ullersma-Caldeira-Leggett-type bath at a finite temperature T_α, the propagating function reads

$$\begin{aligned}&J(q''_{1+}, q''_{2+}, q''_{1-}, q''_{2-}, t; q'_{1+}, q'_{2+}, q'_{1-}, q'_{2-}, 0) = \\ &\frac{1}{N(t)}\exp\left\{\frac{i}{\hbar}\int_0^t {\rm d}s\left[\sum_{\alpha=1}^{2}\left(\frac{1}{2}m_\alpha\dot{q}_{\alpha+}^2(s) - \frac{1}{2}m_\alpha\omega_\alpha^2 q_{\alpha+}^2(s)\right) - c(s)q_{1+}(s)q_{2+}(s)\right]\right\} \\ &\times\exp\left\{-\frac{i}{\hbar}\int_0^t {\rm d}s\left[\sum_{\alpha=1}^{2}\left(\frac{1}{2}m_\alpha\dot{q}_{\alpha-}^2(s) - \frac{1}{2}m_\alpha\omega_\alpha^2 q_{\alpha-}^2(s)\right) - c(s)q_{1-}(s)q_{2-}(s)\right]\right\}\mathcal{F}[q_{1+}, q_{2+}, q_{1-}, q_{2-}],\end{aligned}$$

being $N(t)$ a normalization factor. The influence functional $\mathcal{F}[q_{1+}, q_{2+}, q_{1-}, q_{2-}]$ is given by

$$\begin{aligned}\mathcal{F}[q_{1+}, q_{2+}, q_{1-}, q_{2-}] = \prod_{\alpha=1}^{2} \exp\Bigg(-\frac{\mathrm{i}m_\alpha}{2\hbar}\Bigg\{(q'_{\alpha+} + q'_{\alpha-})\int_0^t \mathrm{d}s\, \gamma_\alpha(s)[q_{\alpha+}(s) - q_{\alpha-}(s)] \\ + \int_0^t \mathrm{d}s \int_0^s \mathrm{d}u\, \gamma_\alpha(s-u)[\dot{q}_{\alpha+}(u) + \dot{q}_{\alpha-}(u)][q_{\alpha+}(s) - q_{\alpha-}(u)]\Bigg\}\Bigg) \\ \times \exp\left\{-\frac{1}{\hbar}\int_0^t \mathrm{d}s \int_0^s \mathrm{d}u\, K_\alpha(u-s)[q_{\alpha+}(s) - q_{\alpha-}(s)][q_{\alpha+}(u) - q_{\alpha-}(u)]\right\},\end{aligned} \tag{66}$$

and $\gamma_\alpha(s)$ and $K_\alpha(s)$ stands for the damping and noise kernels, which are given by

$$\gamma_\alpha(s) = \frac{2}{m_\alpha}\int_0^\infty \frac{\mathrm{d}\omega_\alpha}{\pi}\frac{J_\alpha(\omega_\alpha)}{\omega_\alpha}\cos(\omega_\alpha s), \tag{67}$$

$$K_\alpha(s) = \int_0^\infty \frac{\mathrm{d}\omega_\alpha}{\pi} J_\alpha(\omega_\alpha)\coth\left(\frac{\hbar\beta_\alpha\omega_\alpha}{2}\right)\cos(\omega_\alpha s), \tag{68}$$

being $J_\alpha(\omega_\alpha)$ the spectral density. The complete dynamics depend on the characteritics of the spectral density. For the present analysis, $J_\alpha(\omega_\alpha)$ were chosen as spectral densities with Ohmic dissipation with a cutoff frequencies $\omega_{\alpha\mathrm{D}}$.

As before, the mean value of the phonon number in the mechanical mode $\langle\hat{n}(t)\rangle$ is utilized as the cooling witness. In terms of the second moments of the position $\langle\hat{q}_1^2\rangle$ and momentum $\langle\hat{p}_1^2\rangle$, it is given by

$$\langle\hat{n}\rangle(t) = \frac{1}{2\hbar\omega_1}\left[\frac{\langle\hat{p}_1^2\rangle(t)}{m_1} + m_1\omega_1^2\langle\hat{q}_1^2\rangle(t)\right] - \frac{1}{2}, \tag{69}$$

where the index 1 refers to the mechanical mode. More details about calculations of the propagator, noise kernels and the second moments can be found in Refs. [50, 51].

Measuring cooling or heating is related to the temperature of the considered system. The temperature of a microscopic quantum system with a single degree of freedom is defined on its steady state which is in thermal equilibrium with its finite-temperature environment. In that case, the mean phonon value characterizes well the temperature of the oscillator. Nonetheless, the presence of the counter-rotating terms in the non-Markovian case could generate some squeezing of the mechanical oscillator in its long-time steady state, and there is no apparent reason why the mean phonon value could characterize well the cooling. This is in contrast to the case of the Born-Markovian dynamics, where one can regard this squeezing as a rapid oscillatory effect that could be neglected. In the exact non-Markovian effect, there is no reason to deem that the effect of this term could be ruled out. Squeezing would cause the long-time steady state to deviate from a thermal equilibrium state. Hence, these last considerations may suggest that the mean phonon value is insufficient in characterizing cooling. However, the squeezing parameter both in the Markovian case and in the non-Markovian case remains almost equal as is explained below. Another meaningful mean value to characterize cooling is the entropy of the system [10], this is calculated below to confirm the efficiency of the cooling processes [43].

To calculate the second moments involved in the phonon number in Eq. (69), the half sum and difference coordinates are introduced to simplify the above expressions and subsequent calculations as [50, 51, 52]

$$Q_\alpha = \frac{1}{2}(q_{\alpha+} + q_{\alpha-}), \qquad q_\alpha = q_{\alpha+} - q_{\alpha-}, \tag{70}$$

where the Jacobian of the coordinates transformation is equal to one. Therefore, the differential equations of motion for the coordinates Q_i and q_i take the form

$$\begin{aligned}\ddot{Q}_{1,2}(s) + \omega_{1,2}^2 Q_{1,2}(s) + \frac{c(s)}{m_{1,2}}Q_{2,1}(s) + \frac{\mathrm{d}}{\mathrm{d}s}\int_0^s \mathrm{d}u\, \gamma_{1,2}(s-u)Q_{1,2}(u) = 0, \\ \ddot{q}_{1,2}(s) + \omega_{1,2}^2 q_{1,2}(s) + \frac{c(s)}{m_{1,2}}q_{2,1}(s) - \frac{\mathrm{d}}{\mathrm{d}s}\int_s^t \mathrm{d}u\, \gamma_{1,2}(u-s)q_{1,2}(u) = 0,\end{aligned} \tag{71}$$

and have the following boundary conditions

$$Q_i(s) = \begin{cases} Q'_i, & s = 0 \\ Q''_i, & s = t \end{cases}, \qquad q_i(s) = \begin{cases} q'_i, & s = 0 \\ q''_i, & s = t \end{cases}. \tag{72}$$

Hence, the solution of Eqs. (71) can be expressed as

$$\begin{aligned} Q_1(t,s) &= U_1(t,s)Q_1' + U_2(t,s)Q_1'' + U_3(t,s)Q_2' + U_4(t,s)Q_2'', \\ Q_2(t,s) &= V_1(t,s)Q_2' + V_2(t,s)Q_2'' + V_3(t,s)Q_1' + V_4(t,s)Q_1'', \\ q_1(t,s) &= u_1(t,s)q_1' + u_2(t,s)q_1'' + u_3(t,s)q_2' + u_4(t,s)q_2'', \\ q_2(t,s) &= v_1(t,s)q_2' + v_2(t,s)q_2'' + v_3(t,s)q_1' + v_4(t,s)q_1'', \end{aligned} \tag{73}$$

with the initial conditions

$$Q_i(0) = q_i(0) = 1, \qquad \dot{Q}_i(0) = \dot{q}_i(0) = 1, \qquad Q_i(0) = q_i(0) = 0, \quad \text{and} \quad \dot{Q}_i(0) = \dot{q}_i(0) = 0.$$

The auxiliary functions $U_i(t,s)$, $V_i(t,s)$, $u_i(t,s)$, $v_i(t,s)$, in terms of the functions of the solution of the initial condition problem $\varphi_i(s)$, $\phi_i(s)$, $\nu_i(s)$ and $\vartheta_i(s)$, are given by [50, 51]

$$\begin{aligned} U_1(t,s) = \varphi_1(s) &- \frac{\varphi_1(t)\varphi_2(s)\phi_2(t)}{\varphi_2(t)\phi_2(t) - \varphi_4(t)\phi_4(t)} - \frac{\varphi_2(t)\phi_3(t)\varphi_4(s)}{\varphi_2(t)\phi_2(t) - \varphi_4(t)\phi_4(t)} \\ &+ \frac{\varphi_2(s)\phi_3(t)\varphi_4(t)}{\varphi_2(t)\phi_2(t) - \varphi_4(t)\phi_4(t)} + \frac{\varphi_1(t)\varphi_4(s)\phi_4(t)}{\varphi_2(t)\phi_2(t) - \varphi_4(t)\phi_4(t)}, \end{aligned} \tag{74}$$

$$U_2(t,s) = \frac{\varphi_2(s)\phi_2(t)}{\varphi_2(t)\phi_2(t) - \varphi_4(t)\phi_4(t)} - \frac{\varphi_4(s)\phi_4(t)}{\varphi_2(t)\phi_2(t) - \varphi_4(t)\phi_4(t)}, \tag{75}$$

$$\begin{aligned} U_3(t,s) = \varphi_3(s) &- \frac{\varphi_2(s)\phi_2(t)\varphi_3(t)}{\varphi_2(t)\phi_2(t) - \varphi_4(t)\phi_4(t)} - \frac{\phi_1(t)\varphi_2(t)\varphi_4(s)}{\varphi_2(t)\phi_2(t) - \varphi_4(t)\phi_4(t)} \\ &+ \frac{\phi_1(t)\varphi_2(s)\varphi_4(t)}{\varphi_2(t)\phi_2(t) - \varphi_4(t)\phi_4(t)} + \frac{\varphi_3(t)\varphi_4(s)\phi_4(t)}{\varphi_2(t)\phi_2(t) - \varphi_4(t)\phi_4(t)}, \end{aligned} \tag{76}$$

$$U_4(t,s) = \frac{\varphi_2(t)\varphi_4(s)}{\varphi_2(t)\phi_2(t) - \varphi_4(t)\phi_4(t)} - \frac{\varphi_2(s)\phi_4(t)}{\varphi_2(t)\phi_2(t) - \varphi_4(t)\phi_4(t)}, \tag{77}$$

$$\begin{aligned} V_1(t,s) = \phi_1(s) &- \frac{\phi_1(t)\varphi_2(t)\phi_2(s)}{\varphi_2(t)\phi_2(t) - \varphi_4(t)\phi_4(t)} - \frac{\phi_2(t)\varphi_3(t)\phi_4(s)}{\varphi_2(t)\phi_2(t) - \varphi_4(t)\phi_4(t)} \\ &+ \frac{\phi_1(t)\varphi_4(t)\phi_4(s)}{\varphi_2(t)\phi_2(t) - \varphi_4(t)\phi_4(t)} + \frac{\phi_2(s)\varphi_3(t)\phi_4(t)}{\varphi_2(t)\phi_2(t) - \varphi_4(t)\phi_4(t)}, \end{aligned} \tag{78}$$

$$V_2(t,s) = \frac{\varphi_2(t)\phi_2(s)}{\varphi_2(t)\phi_2(t) - \varphi_4(t)\phi_4(t)} - \frac{\varphi_4(t)\phi_4(s)}{\varphi_2(t)\phi_2(t) - \varphi_4(t)\phi_4(t)}, \tag{79}$$

$$\begin{aligned} V_3(t,s) = \phi_3(s) &- \frac{\varphi_2(t)\phi_2(s)\varphi_3(t)}{\varphi_2(t)\phi_2(t) - \varphi_4(t)\phi_4(t)} - \frac{\varphi_1(t)\phi_2(t)\phi_4(s)}{\varphi_2(t)\phi_2(t) - \varphi_4(t)\phi_4(t)} \\ &+ \frac{\phi_3(t)\varphi_4(t)\phi_4(s)}{\varphi_2(t)\phi_2(t) - \varphi_4(t)\phi_4(t)} + \frac{\varphi_1(t)\phi_2(s)\phi_4(t)}{\varphi_2(t)\phi_2(t) - \varphi_4(t)\phi_4(t)}, \end{aligned} \tag{80}$$

$$V_4(t,s) = \frac{\varphi_2(t)\phi_2(s)}{\varphi_2(t)\phi_2(t) - \varphi_4(t)\phi_4(t)} - \frac{\varphi_4(t)\phi_4(s)}{\varphi_2(t)\phi_2(t) - \varphi_4(t)\phi_4(t)}, \tag{81}$$

$$\begin{aligned} u_1(t,s) = \nu_1(s) &- \frac{\nu_1(t)\nu_2(s)\vartheta_2(t)}{\nu_2(t)\vartheta_2(t) - \nu_4(t)\vartheta_4(t)} - \frac{\nu_2(t)\vartheta_3(t)\nu_4(s)}{\nu_2(t)\vartheta_2(t) - \nu_4(t)\vartheta_4(t)} \\ &+ \frac{\nu_2(s)\vartheta_3(t)\nu_4(t)}{\nu_2(t)\vartheta_2(t) - \nu_4(t)\vartheta_4(t)} + \frac{\nu_1(t)\nu_4(s)\vartheta_4(t)}{\nu_2(t)\vartheta_2(t) - \nu_4(t)\vartheta_4(t)}, \end{aligned} \tag{82}$$

$$u_2(t,s)=\frac{\nu_2(s)\vartheta_2(t)}{\nu_2(t)\vartheta_2(t)-\nu_4(t)\vartheta_4(t)}-\frac{\nu_4(s)\vartheta_4(t)}{\nu_2(t)\vartheta_2(t)-\nu_4(t)\vartheta_4(t)}, \tag{83}$$

$$\begin{aligned}u_3(t,s)=\nu_3(s)&-\frac{\nu_2(s)\vartheta_2(t)\nu_3(t)}{\nu_2(t)\vartheta_2(t)-\nu_4(t)\vartheta_4(t)}-\frac{\vartheta_1(t)\nu_2(t)\nu_4(s)}{\nu_2(t)\vartheta_2(t)-\nu_4(t)\vartheta_4(t)}\\&+\frac{\vartheta_1(t)\nu_2(s)\nu_4(t)}{\nu_2(t)\vartheta_2(t)-\nu_4(t)\vartheta_4(t)}+\frac{\nu_3(t)\nu_4(s)\vartheta_4(t)}{\nu_2(t)\vartheta_2(t)-\nu_4(t)\vartheta_4(t)},\end{aligned} \tag{84}$$

$$u_4(t,s)=\frac{\nu_2(t)\nu_4(s)}{\nu_2(t)\vartheta_2(t)-\nu_4(t)\vartheta_4(t)}-\frac{\nu_2(s)\vartheta_4(t)}{\nu_2(t)\vartheta_2(t)-\nu_4(t)\vartheta_4(t)}, \tag{85}$$

$$\begin{aligned}v_1(t,s)=\vartheta_1(s)&-\frac{\vartheta_1(t)\nu_2(t)\vartheta_2(s)}{\nu_2(t)\vartheta_2(t)-\nu_4(t)\vartheta_4(t)}-\frac{\vartheta_2(t)\nu_3(t)\vartheta_4(s)}{\nu_2(t)\vartheta_2(t)-\nu_4(t)\vartheta_4(t)}\\&+\frac{\vartheta_1(t)\nu_4(t)\vartheta_4(s)}{\nu_2(t)\vartheta_2(t)-\nu_4(t)\vartheta_4(t)}+\frac{\vartheta_2(s)\nu_3(t)\vartheta_4(t)}{\nu_2(t)\vartheta_2(t)-\nu_4(t)\vartheta_4(t)},\end{aligned} \tag{86}$$

$$v_2(t,s)=\frac{\nu_2(t)\vartheta_2(s)}{\nu_2(t)\vartheta_2(t)-\nu_4(t)\vartheta_4(t)}-\frac{\nu_4(t)\vartheta_4(s)}{\nu_2(t)\vartheta_2(t)-\nu_4(t)\vartheta_4(t)}, \tag{87}$$

$$\begin{aligned}v_3(t,s)=\vartheta_3(s)&-\frac{\nu_2(t)\vartheta_2(s)\nu_3(t)}{\nu_2(t)\vartheta_2(t)-\nu_4(t)\vartheta_4(t)}-\frac{\nu_1(t)\vartheta_2(t)\vartheta_4(s)}{\nu_2(t)\vartheta_2(t)-\nu_4(t)\vartheta_4(t)}\\&+\frac{\vartheta_3(t)\nu_4(t)\vartheta_4(s)}{\nu_2(t)\vartheta_2(t)-\nu_4(t)\vartheta_4(t)}+\frac{\nu_1(t)\vartheta_2(s)\vartheta_4(t)}{\nu_2(t)\vartheta_2(t)-\nu_4(t)\vartheta_4(t)},\end{aligned} \tag{88}$$

$$v_4(t,s)=\frac{\nu_2(t)\vartheta_2(s)}{\nu_2(t)\vartheta_2(t)-\nu_4(t)\vartheta_4(t)}-\frac{\nu_4(t)\vartheta_4(s)}{\nu_2(t)\vartheta_2(t)-\nu_4(t)\vartheta_4(t)}. \tag{89}$$

Therefore, in terms of the solutions of the initial condition problem with φ_i, ϕ_i, ν_i and ϑ_i, the equations of motion are transformed as [50, 51]

$$\begin{aligned}&\ddot{\varphi}_{1,3}(s)+\omega_1^2\varphi_{1,3}(s)+\frac{c(s)}{m_1}\phi_{3,1}(s)+\frac{\mathrm{d}}{\mathrm{d}s}\int_0^s \mathrm{d}u\,\gamma_1(s-u)\varphi_{1,3}(u)=0,\\&\ddot{\varphi}_{2,4}(s)+\omega_1^2\varphi_{2,4}(s)+\frac{c(s)}{m_1}\phi_{4,2}(s)+\frac{\mathrm{d}}{\mathrm{d}s}\int_0^s \mathrm{d}u\,\gamma_1(s-u)\varphi_{2,4}(u)=0,\\&\ddot{\phi}_{1,3}(s)+\omega_2^2\phi_{1,3}(s)+\frac{c(s)}{m_2}\varphi_{3,1}(s)+\frac{\mathrm{d}}{\mathrm{d}s}\int_0^s \mathrm{d}u\,\gamma_2(s-u)\phi_{1,3}(u)=0,\\&\ddot{\phi}_{2,4}(s)+\omega_2^2\phi_{2,4}(s)+\frac{c(s)}{m_2}\varphi_{4,2}(s)+\frac{\mathrm{d}}{\mathrm{d}s}\int_0^s \mathrm{d}u\,\gamma_2(s-u)\phi_{2,4}(u)=0,\end{aligned} \tag{90}$$

$$\begin{aligned}&\ddot{\nu}_{1,3}(s)+\omega_1^2\nu_{1,3}(s)+\frac{c(s)}{m_1}\vartheta_{3,1}(s)-\frac{\mathrm{d}}{\mathrm{d}s}\int_s^t \mathrm{d}u\,\gamma_1(u-s)\nu_{1,3}(u)=0,\\&\ddot{\nu}_{2,4}(s)+\omega_1^2\nu_{2,4}(s)+\frac{c(s)}{m_1}\vartheta_{4,2}(s)-\frac{\mathrm{d}}{\mathrm{d}s}\int_s^t \mathrm{d}u\,\gamma_1(u-s)\nu_{2,4}(u)=0,\\&\ddot{\vartheta}_{1,3}(s)+\omega_2^2\vartheta_{1,3}(s)+\frac{c(s)}{m_2}\nu_{3,1}(s)-\frac{\mathrm{d}}{\mathrm{d}s}\int_s^t \mathrm{d}u\,\gamma_2(u-s)\vartheta_{1,3}(u)=0,\\&\ddot{\vartheta}_{2,4}(s)+\omega_2^2\vartheta_{2,4}(s)+\frac{c(s)}{m_2}\nu_{4,2}(s)-\frac{\mathrm{d}}{\mathrm{d}s}\int_s^t \mathrm{d}u\,\gamma_2(u-s)\vartheta_{2,4}(u)=0.\end{aligned} \tag{91}$$

The dissipation kernels used in Eqs. (90-91), for the mechanical and electromagnetic mode, are given by

$$\gamma_1(s) = \gamma_1\omega_{1\mathrm{D}}e^{-\omega_{1\mathrm{D}}s}, \qquad \gamma_2(s) = \gamma_2\omega_{2\mathrm{D}}e^{-\omega_{2\mathrm{D}}s}, \tag{92}$$

which corresponds to the dissipation kernels that arise from the spectral density with a Drude cutoff frequency in Eq. (23). These dissipation kernels have been chosen because they reduce Eqs. (90) and (91) from four integro-differential equations to six differential equations.

Optimization Algorithm in the non-Markovian case.—The condition to minimize, the mean phonon number in Eq. (69), is given in terms of the second moments of the position and momentum operators, which in turn are given in terms of the functions φ_i, ϕ_i, ν_i and ϑ_i. This makes quite tedious the calculation of the "initial" conditions for the costate equations. The optimization algorithm uses the same steps as before, but with a modification in the third step. For the non-Markovian case, the "initial" (final) conditions for the costate equations [Eq. (56)] are given, in terms of the seconds moments and the auxiliary function introduced in Eqs. (90) and (91), by

$$\begin{aligned} p_{\varphi_j}(t_f) &= \frac{1}{2}\left(\frac{\partial\langle\hat{p}^2\rangle}{\partial\varphi_j} + \frac{\partial\langle\hat{q}^2\rangle}{\partial\varphi_j}\right), & p_{\varphi_{j\mathrm{p}}}(t_f) &= \frac{1}{2}\left(\frac{\partial\langle\hat{p}^2\rangle}{\partial\varphi_{j\mathrm{p}}} + \frac{\partial\langle\hat{q}^2\rangle}{\partial\varphi_{j\mathrm{p}}}\right), \\ p_{\phi_j}(t_f) &= \frac{1}{2}\left(\frac{\partial\langle\hat{p}^2\rangle}{\partial\phi_j} + \frac{\partial\langle\hat{q}^2\rangle}{\partial\phi_j}\right), & p_{\phi_{j\mathrm{p}}}(t_f) &= \frac{1}{2}\left(\frac{\partial\langle\hat{p}^2\rangle}{\partial\phi_{j\mathrm{p}}} + \frac{\partial\langle\hat{q}^2\rangle}{\partial\phi_{j\mathrm{p}}}\right), \end{aligned} \tag{93}$$

$$p_{\nu_j}(t_f) = \frac{1}{2}\left[\frac{\partial\langle\hat{p}^2\rangle}{\partial\nu_j} + \frac{\partial\langle\hat{q}^2\rangle}{\partial\nu_j} + \sum_{i=1}^{4}\left(\frac{\partial\langle\hat{p}^2\rangle}{\partial\nu_{ji}} + \frac{\partial\langle\hat{q}^2\rangle}{\partial\nu_{ji}}\right)\nu_{i_l} + \sum_{i=1,i\neq j}^{4}\left(\frac{\partial\langle\hat{p}^2\rangle}{\partial\nu_{ij}} + \frac{\partial\langle\hat{q}^2\rangle}{\partial\nu_{ij}}\right)\nu_{j_r}\right], \tag{94}$$

$$p_{\vartheta_j}(t_f) = \frac{1}{2}\left[\frac{\partial\langle\hat{p}^2\rangle}{\partial\vartheta_j} + \frac{\partial\langle\hat{q}^2\rangle}{\partial\vartheta_j} + \sum_{i=1}^{4}\left(\frac{\partial\langle\hat{p}^2\rangle}{\partial\vartheta_{ji}} + \frac{\partial\langle\hat{q}^2\rangle}{\partial\vartheta_{ji}}\right)\vartheta_{i_l} + \sum_{i=1,i\neq j}^{4}\left(\frac{\partial\langle\hat{p}^2\rangle}{\partial\vartheta_{ij}} + \frac{\partial\langle\hat{q}^2\rangle}{\partial\vartheta_{ij}}\right)\vartheta_{i_r}\right], \tag{95}$$

with $j = 1, 2, 3, 4$ and $\nu_{i_{l,r}}$ and $\vartheta_{i_{l,r}}$ given by

$$\begin{aligned} \nu_{i_r} &= \int_0^t \mathrm{d}s \int_0^s \mathrm{d}u\, K_1(u-s)u_i(s), & \vartheta_{i_r} &= \int_0^t \mathrm{d}s \int_0^s \mathrm{d}u\, K_2(u-s)v_i(s), \\ \nu_{i_l} &= \int_0^t \mathrm{d}s \int_0^s \mathrm{d}u\, K_1(u-s)u_i(u), & \vartheta i_l &= \int_0^t \mathrm{d}s \int_0^s \mathrm{d}u\, K_2(u-s)v_i(u), \end{aligned} \tag{96}$$

where $K_i(s)$ is the noise kernel generated by the dissipation kernels in Eqs. (92) and calculated with Eq. (68) [51].

Table 1 summarizes the results under Markovian and non-Markovian dynamics for the minimum phonon number at the cooling time t_{cool}. To compare to the same theory and equations of motion, the Markovian approximation is taking by a high cutoff frequency $\omega_{\mathrm{D}} = 10\omega_{\mathrm{m}}$ and the non-Markovian as $\omega_{\mathrm{D}} = \omega_{\mathrm{m}}$. This comparison is shown in Fig. 5 for different values of dissipation rate γ in the mechanical resonator. The insets of Fig. 5 show a magnification in the final time, thus allowing for a better comparison between the three cooling scenarios: Markovian case [Eqs. (37-52)], Markovian case with $\omega_{\mathrm{D}} = 10\omega_{\mathrm{m}}$ using the Eqs. (90-91) and non-Markovian case.

TABLE 1: Minimum phonon number at time $t = 0.55\tau_{\mathrm{m}}$ using the coupling function $g(t)$.

Dissipation rates	$\langle\hat{n}(t_f)\rangle$				Percentage
	Markovian ($\omega_{\mathrm{D}} \to \infty$)	Markovian ($\omega_{\mathrm{D}} = 10\omega_{\mathrm{m}}$)	Non-Markovian ($\omega_{\mathrm{D}} = \omega_{\mathrm{m}}$)	Non-Markovian Optimized	
$\kappa = \gamma = 10^{-6}\omega_{\mathrm{m}}$	9.03×10^{-3}	8.96×10^{-3}	8.86×10^{-3}	3.43×10^{-3}	61.29 %
$\kappa = \gamma = 10^{-5}\omega_{\mathrm{m}}$	1.04×10^{-2}	1.03×10^{-2}	1.02×10^{-2}	4.79×10^{-3}	53.04 %
$\kappa = \gamma = 10^{-4}\omega_{\mathrm{m}}$	3.28×10^{-2}	3.30×10^{-2}	2.39×10^{-2}	1.83×10^{-2}	23.43 %
$\kappa = \gamma = 10^{-3}\omega_{\mathrm{m}}$	2.61×10^{-1}	2.62×10^{-1}	1.61×10^{-1}	1.53×10^{-1}	4.97 %
$\kappa = \gamma = 10^{-2}\omega_{\mathrm{m}}$	2.45	2.50	1.52	1.50	1.32 %
$\kappa = \gamma = 10^{-1}\omega_{\mathrm{m}}$	21.12	24.77	14.64	13.52	0.68 %

The three first columns in Table 1 show that under non-Markovian dynamics the mean phonon number is smaller in than under Markovian dynamics, and that when dissipation increases, improvement of the results is more noticeable.

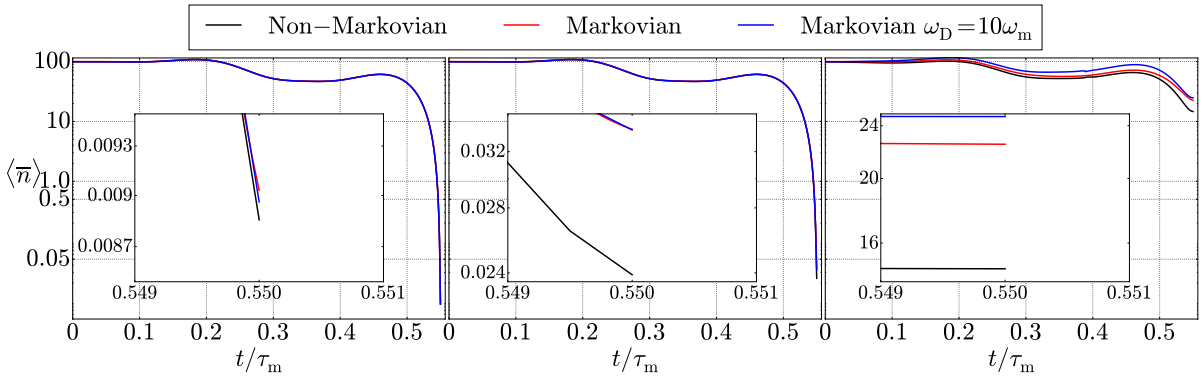

FIGURE 5: Comparison of the cooling dynamics between the three processes, Markovian, non-Markovian and Markovian with $\omega_D = 10\omega_m$, for different parameters for dissipation, from left to right, $\gamma = 10^{-6}\omega_m$, $\gamma = 10^{-4}\omega_m$ and $\gamma = 10^{-1}\omega_m$. The initial parameters are $n_{th} = 100$, $n_{cav} = 0$. Insets: Magnification in the final time $t_{cool} = 0.55\tau_m$.

However, the coupling function $g(t)$ used in these three processes was found through an optimization process in the Markovian approximation. Performing the optimization process to reach the optimal coupling function under non-Markovian dynamics gives as result the optimal coupling function in the non-Markovian dynamics depicted in the inset of Fig. 6 (black line). Optimal coupling $g_{NM}(t)$ has the same behaviour of the coupling function $g(t)$ found in the Markovian case and both are almost identical. Despite of the minimum variation in the coupling function, there is a significant change in the minimum phonon number. The minimum phonon number found after optimization for different values of the dissipation is shown in Table 1.

According to results in Eq. (33), the minimum phonon number in the non-Markovian dynamics is $n_D \approx 0.38 n_M$. Although there is a difference of 0.13 with the results at equilibrium, this result agrees with Eq. (33). The difference being that the time has been chosen at hand and may not be the optimal time. Moreover, results at equilibrium have been found when the dissipation parameter in the mechanical tends to zero whereas for the out-of-equilibrium case $\gamma \neq 0$ was used. Additionally, when dissipation increases, the minimum phonon number does not have a significant decrease, e.g., when the dissipation rate is bigger than 10^{-2}, there is no cooling in the resonator ($\langle \hat{n}(t_f) \rangle > 1$).

Last results show that non-Markovian character of the dynamics plays an important role in sideband cooling and suggest that the non-Markovian character should be included to reach more realistic results in many different kind of systems. Another key result here is the robustness of the optimization process in the non-Markovian case [27].

Squeezing generation is analyzed next to confirm that the mean value of the phonon number characterizes the cooling and consequently describes well the temperature of the oscillator.

Squeezing Generation by Non-Markovian Dynamics

Under non-Markovian dynamics, in general, the system of interest does not always thermalize and part of its quantum coherence could be preserved in the steady state [2, 56]. In Ref. [2], it is shown that even at thermal equilibrium, non-Markovian dynamics allow for (i) generating squeezing in a single harmonic mode that induces deviations from the canonical thermal state and (ii) the presence of entanglement between two harmonic modes [51, 7]. As discussed above, measuring cooling based on the mean phonon number may be problematic because the final state may not be thermal.

For the case at hand, interest is in the mechanical mode that is assumed to be in a thermal state at $t = 0$ with $k_B T/\hbar\omega_m \gg 1$. During the subsequent ultrafast dynamics, the time-dependent character of the coupling may squeeze the normal modes of the optomechanical systems and, certainly, takes the system into a non-thermal state. Note that this time-depedent-coupling-induced squeezing is also present in the Markovian case considered in Ref. [11] and in all of the original proposal of sideband cooling [22, 57].

A possible way to characterize the deviations from a thermal state is the $g^2(t)$ correlation function; however, due to the Gaussian character of the state of the mechanical and optical states, and for the present purposes, an equivalent

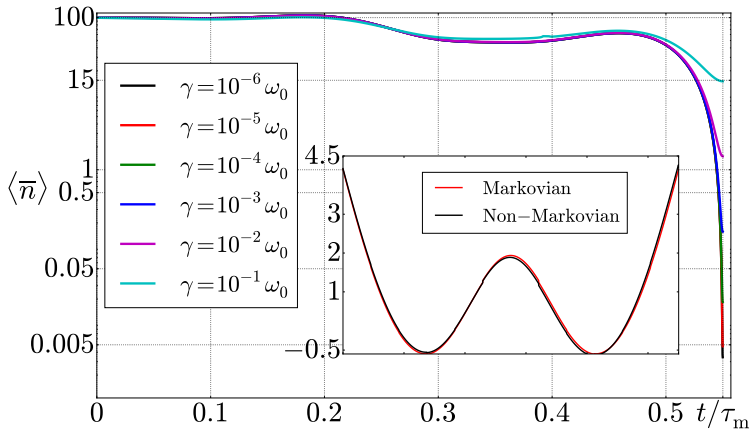

FIGURE 6: Non-Markovian optimal dynamics of cooling. The initial parameters are $n_{\rm T} = 100$, $n_{\rm cav} = 0$. Inset: The optimal control pulse for the coupling rate $g_{\rm NM}(t)$ compare with the optimal control pulse for the coupling rate $g(t)$ shown in Fig. 3. The y-axis is in logarithmic scale.

calculation to the $g^{(2)}$ function is the direct calculation of the squeezing parameter $r(t)$ defined as

$$r = \frac{1}{2}\log\left(\frac{\langle \Delta q\rangle^2}{\langle \Delta p\rangle^2}\right), \tag{97}$$

being $\langle \Delta q\rangle^2$ and $\langle \Delta p\rangle^2$ the dispersion of the position and momentum, respectively.

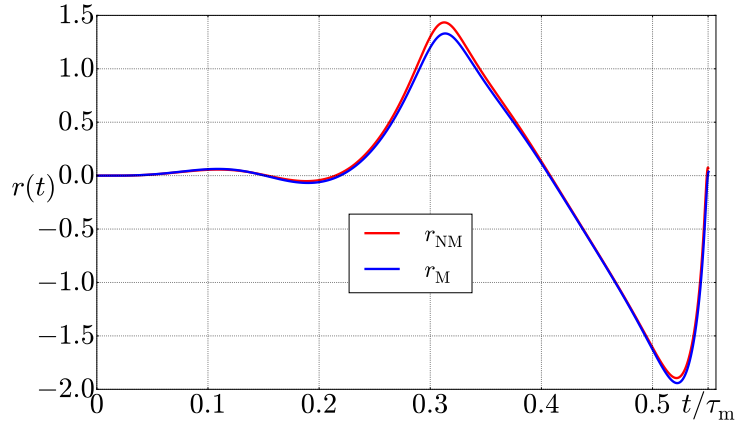

FIGURE 7: Squeezing parameter $r(t)$ for the cooling protocol depicted by the black curve in Fig. 3 under Markovian [blue curve, $r_{\rm M}(t)$] and non-Markovian [red curve, $r_{\rm NM}(t)$] dynamics. The parameters are $\gamma = 10^{-6}\omega_{\rm m}$, $\kappa = 2.15 \times 10^{-4}\omega_{\rm c}$, $n_{\rm T} = 100$ and $n_{\rm cav} = 0$.

For the parameters used for the red curve and blue curve in the inset of Fig. 3, Fig. 7 depicts the time dependence of the squeezing parameter of the mechanical mode state $r(t)$. Because the initial state is thermal at high temperature and no initial system-bath correlations are considered, the initial squeezing parameter is $r(0) = 0$. The subsequent time-modulation of the coupling induces squeezing that goes very close to zero at the end of the cooling protocol. Specifically, $r_{\rm NM}(t_{\rm cool}) = 7.193 \times 10^{-2}$ and $r_{\rm M}(t_{\rm cool}) = 3.572 \times 10^{-2}$.

Therefore, non-Markovian dynamics generate more squeezing than the Markovian one; however, due to the parameter regime, the excess of squeezing $\Delta r(t) = r_{\rm NM}(t) - r_{\rm M}(t)$ at the cooling time $t_{\rm cool}$ is very small $\Delta r(t_{\rm cool}) = 3.621 \times 10^{-2}$. Thus, it is safe to consider the mean phonon number as an measure of cooling. Because in some cases

the phonon number is not taken as a good measure of the cooling, calculations of the entropy transfer are performed to also confirm that the initial energy in the mechanical mode is transfer to the optical mode.

Entropy Transfer

Interest concerns how to reduce the phonon number in the mechanical mode to achieve, as soon as possible, a state near to the ground state. An alternative cooling witness is the entropy at the mechanical mode. If the entropy of the mechanical mode decreases as the optical mode entropy increases, the effective temperature of the mechanical mode decreases, i.e., mechanical mode is cooled although an absolute value for the temperature is not given. Figure 8 depicts the von Newman entropy given by [10]

$$S(x) = \left(x + \frac{1}{2}\right)\log\left(x + \frac{1}{2}\right) - \left(x - \frac{1}{2}\right)\log\left(x - \frac{1}{2}\right), \qquad x = \sqrt{\langle q^2\rangle\langle p^2\rangle - \langle pq + qp\rangle^2/4}, \tag{98}$$

for the mechanical and the optical mode as a function of time.

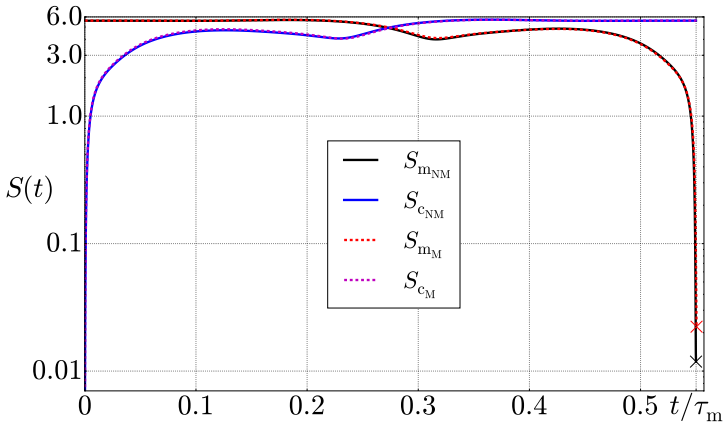

FIGURE 8: von Neumann entropy of the both mechanical (S_{m}) and optical mode (S_{c}). Parameters as in Fig. 1. Continuous lines for non-Markovian dynamics ($S_{\mathrm{m_{NM}}}$ and $S_{\mathrm{c_{NM}}}$) and dashed lines for Markovian dynamics ($S_{\mathrm{m_M}}$ and $S_{\mathrm{c_M}}$) when $\omega_{\mathrm{D}} \to \infty$.

Cooling at this level is guaranteed by the fact that the entropy in the mechanical mode decreases; specifically, it decreases from $S_{\mathrm{m}}(0) = 5.6101$ to $S_{\mathrm{m}}(t_{\mathrm{cool}}) = 2.23 \times 10^{-2}$ in the Markovian case and to $S_{\mathrm{m}}(t_{\mathrm{cool}}) = 2.19 \times 10^{-2}$ in the non-Markovian case. Thus, the systems sits very close to its ground state (zero entropy). For the cavity mode, it varies from $S_{\mathrm{c}}(0) = 0$ to $S_{\mathrm{c}}(t_{\mathrm{cool}}) = 5.601$ in the Markovian case and to $S_{\mathrm{c}}(t_{\mathrm{cool}}) = 5.607$ in the non-Markovian. Although for this set of parameters, the entropy difference is not substantial, from the analysis above, it is clear that if the dissipative rate γ increases, then the entropy difference does so.

CONCLUSIONS

When non-Markovian dynamics are considered in the optimal cooling of resonators by sideband cooling, cooling process is more effective than in the Markovian approximation. Therefore, previous works on sideband cooling [15, 16, 11, 58] may benefict from the non-Markovian correlations. According to Figs. 3 and 6, ultrafast cooling requieres ultrastrong optomechanical, $g(t) > 10^{-2}$. However, a tremendous increase in g was demonstrated recently in an experiment by Teufel *et al.* [9]. This has brought g within a factor of 10 of ω_0, which demonstrated that in the future, the increase of the coupling g is feasible. Moreover, if the ultrafast condition is relaxed, then the coupling amplitude decreases [27], e.g., if cooling is required to occur after of one period of the mechanical oscillation, then the amplitude of g decreases, roughly, by an order of magnitude. The decrease of amplitude favors the current implementation of the present optimal cooling approach as well as guaranties that the optomechanical coupling is still in the linear regime.

On the technical side, the optimal protocol presented here would benefit from a reformulation in phase space [59, 60] because the boundary problem translate by construction into initial condition problem [60, 61]. This would also pave the way for the extension of the present protocol for analyzing non-linear systems in the semiclassical regime [61, 62]. Work along tis line is in progress.

ACKNOWLEDGMENTS

This work was supported by *Comité para el Desarrollo de la Investigación* (CODI) of Universidad de Antioquia, Colombia under the *Estrategia de Sostenibilidad* and under contract number 2015-7631 and by the *Departamento Administrativo de Ciencia, Tecnología e Innovación* (COLCIENCIAS) of Colombia under the contract number FP44842-119-2016.

REFERENCES

[1] D. Kleckner and D. Bouwmeester, Nature **444**, 75–78 (2006).
[2] L. A. Pachón, J. F. Triana, D. Zueco, and P. Brumer, arXiv **1401.1418** (2014).
[3] J. Lee, W. Shen, K. Payer, T. P. Burg, and S. R. Manalis, Nano Letters **10**, 2537–2542 (2010).
[4] M. D. LaHaye, O. Buu, B. Camarota, and K. C. Schwab, Science **304**, 74–77 (2004).
[5] B. Abbott, R. Abbott, R. Adhikari, and et. al, New Journal of Physics **11**, p. 073032 (2009).
[6] K. C. Schwab and M. L. Roukes, Physics Today **4**, p. 36 (2005).
[7] F. Galve, L. A. Pachón, and D. Zueco, Phys. Rev. Lett. **105**, p. 180501 (2010).
[8] A. D. O'Connell, M. Hofheinz, and et. al, Nature **464**, 697 – 703 (2010).
[9] J. D. Teufel, T. Donner, D. Li, J. W. Harlow, M. S. Allman, K. Cicak, A. J. Sirois, J. D. Whittaker, K. W. Lehnert, and R. W. Simmonds, Nature **475**, 359–363 (2011).
[10] R. Schmidt, A. Negretti, J. Ankerhold, T. Calarco, and J. T. Stockburger, Phys. Rev. Lett. **107**, p. 130404 (2011).
[11] X. Wang, S. Vinjanampathy, F. W. Strauch, and K. Jacobs, Phys. Rev. Lett. **107**, p. 177204 (2011).
[12] N. Erez, G. Gordon, M. Nest, and G. Kurizki, Nature **452**, 724–727 (2008).
[13] A. E. Allahverdyan, R. S. Gracià, and T. M. Nieuwenhuizen, Phys. Rev. Lett. **93**, p. 260404 (2004).
[14] S. Mancini, D. Vitali, and P. Tombesi, Phys. Rev. Lett. **80**, 688–691 (1998).
[15] F. Marquardt, J. P. Chen, A. A. Clerk, and S. M. Girvin, Phys. Rev. Lett. **99**, p. 093902 (2007).
[16] S. Machnes, J. Cerrillo, M. Aspelmeyer, W. Wieczorek, M. B. Plenio, and A. Retzker, Phys. Rev. Lett. **108**, p. 153601 (2012).
[17] F. Marquardt and S. M. Girvin, Physics **2**, p. 40 (2009).
[18] A. H. Safavi-Naeini, J. Chan, J. T. Hill, S. Grblacher, H. Miao, Y. Chen, M. Aspelmeyer, and O. Painter, New Journal of Physics **15**, p. 035007 (2013).
[19] A. A. Clerk, M. H. Devoret, S. M. Girvin, F. Marquardt, and R. J. Schoelkopf, Rev. Mod. Phys. **82**, 1155–1208 (2010).
[20] M. Aspelmeyer, T. J. Kippenberg, and F. Marquardt, Rev. Mod. Phys. **86**, 1391–1452 (2014).
[21] Y.-S. Park and H. Wang, Nat. Phys **5**, p. 489 (2009).
[22] I. Wilson-Rae, N. Nooshi, W. Zwerger, and T. J. Kippenberg, Phys. Rev. Lett. **99**, p. 093901 (2007).
[23] R. Rivière, S. Deléglise, S. Weis, E. Gavartin, O. Arcizet, A. Schliesser, and T. J. Kippenberg, Phys. Rev. A **83**, p. 063835 (2011).
[24] J. Hofer, A. Schliesser, and T. J. Kippenberg, Phys. Rev. A **82**, p. 031804 (2010).
[25] E. Verhagen, S. Deleglise, S. Weis, A. Schliesser, and T. J. Kippenberg, Nature **482**, 63–67 (2012).
[26] K. Kumar, J. Math. Physics **6**, 1923–1927 (1965).
[27] J. F. Triana, A. F. Estrada, and L. A. Pachón, Phys. Rev. Lett. **116**, p. 183602 (2016).
[28] G. Anetsberger, O. Arcizet, Q. P. Unterreithmeier, R. Riviere, A. Schliesser, E. M. Weig, J. P. Kotthaus, and T. J. Kippenberg, Nat Phys **5**, 909–914 (2008).
[29] L. Tian, M. S. Allman, and R. W. Simmonds, New Journal of Physics **10**, p. 115001 (2008).
[30] R. H. Koch, G. A. Keefe, F. P. Milliken, J. R. Rozen, C. C. Tsuei, J. R. Kirtley, and D. P. DiVincenzo, Phys. Rev. Lett. **96**, p. 127001 (2006).
[31] A. Blais, R.-S. Huang, A. Wallraff, S. M. Girvin, and R. J. Schoelkopf, Phys. Rev. A **69**, p. 062320 (2004).
[32] C. W. Gardiner and M. J. Collett, Phys. Rev. A **31**, 3761–3774Jun (1985).

[33] C. Gardiner and P. Zoller, *Quantum Noise: A Handbook of Markovian and Non-Markovian Quantum Stochastic Methods with Applications to Quantum Optics*, Springer Series in Synergetics (Springer, 2004).
[34] W. Louisell, *Quantum statistical properties of radiation*, Wiley Series in Pure and Applied Optics Series (John Wiley & Sons Canada, Limited, 1973).
[35] L. A. Pachón and P. Brumer, J. Chem. Phys. **141**, p. 174102 (2014).
[36] L. A. Pachon, A. H. Marcus, and A. Aspuru-Guzik, J. Chem. Phys. **142**, p. 212442 (2015), https://doi.org/10.1063/1.4919954 .
[37] D. Kirk, *Optimal Control Theory: An Introduction*, Dover Books on Electrical Engineering (Dover Publications, 2012).
[38] H. Breuer and F. Petruccione, *The Theory of Open Quantum Systems* (OUP Oxford, 2007) Chap. 3.
[39] H. Geering, *Optimal Control with Engineering Applications* (Springer Berlin Heidelberg, 2007).
[40] S. Aniţa, V. Arnăutu, and V. Capasso, *An Introduction to Optimal Control Problems in Life Sciences and Economics: From Mathematical Models to Numerical Simulation with MATLAB®*, Modeling and Simulation in Science, Engineering and Technology (Birkhäuser Boston, 2011).
[41] S. Lenhart and J. Workman, *Optimal Control Applied to Biological Models*, Chapman & Hall/CRC Mathematical and Computational Biology (Taylor & Francis, 2007).
[42] P. Chen and S. Islam, *Optimal Control Models in Finance: A New Computational Approach*, Applied Optimization (Springer US, 2006).
[43] J. F. Triana, A. F. Estrada, and L. A. Pachón, In preparation (2017).
[44] M. Mariantoni, F. Deppe, A. Marx, R. Gross, F. K. Wilhelm, and E. Solano, Phys. Rev. B **78**, p. 104508 (2008).
[45] G. M. Reuther, D. Zueco, F. Deppe, E. Hoffmann, E. P. Menzel, T. Weißl, M. Mariantoni, S. Kohler, A. Marx, E. Solano, R. Gross, and P. Hänggi, Phys. Rev. B **81**, p. 144510 (2010).
[46] M. J. Woolley, G. J. Milburn, and C. M. Caves, New Journal of Physics **10**, p. 125018 (2008).
[47] R. Feynman and F. Vernon, Annals of Physics **24**, 118 – 173 (1963).
[48] H. Grabert, U. Weiss, and P. Talkner, Z. Phys. B **55**, p. 87 (1984).
[49] H. Grabert, P. Schramm, and G.-L. Ingold, Phys. Rep. **168**, p. 115 (1988).
[50] A. F. Estrada, "Efectos no markovianos en la dinámica del entrelazamiento a altas temperaturas," Bachelor's Thesis (Universidad de Antioquia, Medellín, Colombia, 2013).
[51] A. F. Estrada and L. A. Pachon, New J. Phys. **17**, p. 033038 (2015).
[52] L. A. Pachón and P. Brumer, J. Math. Phys. **55** (2014).
[53] A. O. Caldeira and A. J. Leggett, Phys. Rev. Lett. **46**, 211–214 (1981).
[54] A. Caldeira and A. Leggett, Annals of Physics **149**, 374 – 456 (1983).
[55] A. O. Caldeira and A. L. Leggett, Physica A **121**, p. 587 (1983).
[56] H. Xiong, P. Lo, W. Zhang, and F. Nori, Sci. Rep. **5**, p. 13353 (2015).
[57] C.-J. Yang, J.-H. An, H.-G. Luo, Y. Li, and C. H. Oh, Phys. Rev. E **90**, p. 022122 (2014).
[58] Y.-C. Liu, Y.-F. Xiao, X. Luan, and C. W. Wong, Phys. Rev. Lett. **110**, p. 153606 (2013).
[59] T. Dittrich and L. A. Pachón, Phys. Rev. Lett. **102**, p. 150401Apr (2009).
[60] L. Pachón, G.-L. Ingold, and T. Dittrich, Chemical Physics **375**, 209 – 215 (2010).
[61] T. Dittrich, E. A. Gómez, and L. A. Pachón, J. Chem. Phys. **132**, p. 214102 (2010).
[62] L. A. Pachón and P. Brumer, Phys. Chem. Chem. Phys. **14**, p. 10094 (2012).